Original Article

Metabolic endotoxemia promotes neuroinflammation after focal cerebral ischemia

Naohide Kurita[1], Kazuo Yamashiro[1], Takuma Kuroki[1], Ryota Tanaka[2], Takao Urabe[3], Yuji Ueno[1], Nobukazu Miyamoto[1], Masashi Takanashi[1], Hideki Shimura[3], Toshiki Inaba[3], Yuichiro Yamashiro[4], Koji Nomoto[4,5], Satoshi Matsumoto[4,6], Takuya Takahashi[4,7], Hirokazu Tsuji[4,6], Takashi Asahara[4,6] and Nobutaka Hattori[1]

[1]Department of Neurology, Juntendo University School of Medicine, Tokyo, Japan

[2]Division of Neurology, Department of Internal Medicine, Jichi Medical University, Tochigi Japan

[3]Department of Neurology, Juntendo University Urayasu Hospital, Chiba, Japan

[4]Probiotics Research Laboratory, Juntendo University Graduate School of Medicine, Tokyo, Japan

[5]Laboratory of Animal Symbiotic Microorganisms, Department of Molecular Biology, Faculty of Life Science, Tokyo University of Agriculture, Tokyo, Japan

[6]Yakult Central Institute, Tokyo, Japan

[7]Yakult Honsha European Research Center for Microbiology ESV, Gent, Belgium

Corresponding author: Kazuo Yamashiro, MD

Department of Neurology, Juntendo University School of Medicine

2-1-1 Hongo, Bunkyo-ku, Tokyo 113-8421, Japan

Tel: +81 3 3813 3111

Email: kazuo-y@juntendo.ac.jp

Running headline: Metabolic endotoxemia and stroke

Abstract

Lipopolysaccharide (LPS) is a major component of the outer membrane of Gram-negative bacteria and a potent inflammatory stimulus for the innate immune response via toll-like receptor (TLR) 4 activation. Type 2 diabetes is associated with changes in gut microbiota and impaired intestinal barrier functions, leading to translocation of microbiota-derived LPS into the circulatory system, a condition referred to as metabolic endotoxemia. We investigated the effects of metabolic endotoxemia after experimental stroke with transient middle cerebral artery occlusion (MCAO) in a murine model of type 2 diabetes (*db/db*) and phenotypically normal littermates (*db/+*). Compared to *db/+* mice, *db/db* mice exhibited an altered gut microbial composition, increased intestinal permeability, and higher plasma LPS levels. In addition, *db/db* mice presented increased infarct volumes and higher expression levels of LPS, TLR4, and inflammatory cytokines in the ischemic brain, as well as more severe neurological impairments and reduced survival rates after MCAO. Oral administration of a non-absorbable antibiotic modulated the gut microbiota and improved metabolic endotoxemia and stroke outcomes in *db/db* mice; these effects were associated with reduction of LPS levels and neuroinflammation in the ischemic brain. These data suggest that targeting metabolic endotoxemia may be a novel potential therapeutic strategy to improve stroke outcomes.

Keywords: Gram-negative bacteria, lipopolysaccharide, metabolic endotoxemia, stroke, type 2 diabetes.

Introduction

Lipopolysaccharide (LPS), often referred to as endotoxin, is a major component of the outer membrane of Gram-negative bacteria. Lipopolysaccharide is a potent inflammatory stimulus for the innate immune response via toll-like receptor (TLR) 4 activation.[1] Inflammation plays important roles in the development of strokes and is also implicated in the pathophysiology of ischemic lesions, as well as in the overall outcome after stroke.[2] According to the Bruneck Study, an increased plasma LPS level constitutes a substantial risk factor for incident carotid atherosclerosis and cardiovascular disease.[3] Furthermore, a higher plasma LPS level is associated with worse short-term outcomes in patients with acute ischemic stroke.[4] Experimental studies have demonstrated that systemic LPS administration exacerbates brain damage after cerebral ischemia.[5,6]

The human intestine is home to a vast number of bacteria, and the intestinal barrier prevents under physiological conditions, the passage of harmful luminal contents such as LPS.[7] Recently, growing evidence has emerged that chronic exposure of the host to gut microbiota-derived LPS links to metabolic disorders, a condition referred to as metabolic endotoxemia.[8] Alteration of gut microbiota (gut dysbiosis) and impairment of intestinal barrier functions lead to translocation of LPS into the circulatory system and

contribute to the pathogenesis of type 2 diabetes via the activation of proinflammatory cascades in adipose tissues.[8] Furthermore, increased intestinal permeability and increased circulating LPS levels have been reported to contribute to the pathogenesis of nonalcoholic steatohepatitis by inflammatory liver damage.[9] In patients with type 2 diabetes, increased serum levels of LPS and proinflammatory cytokines have been reported.[10] In addition, we have previously demonstrated increased inflammatory marker levels concurrent with gut dysbiosis and higher LPS-binding protein concentrations, which reflect circulating LPS levels.[11] These findings indicate the importance of gut microbiota-derived LPS as a trigger for inflammatory responses in the host in type 2 diabetes.

Stroke commonly occurs in patients with cardiovascular risk factors. Type 2 diabetes is observed in approximately 60% of patients with acute ischemic stroke.[12] Type 2 diabetes is not only associated with a significantly increased stroke risk but also an early progression of ischemic lesions[13] and worse functional outcomes.[14] However, establishment of clinically effective neuroprotective therapies has been challenging.[15,16]

Hence, to study whether metabolic endotoxemia could be a therapeutic target to improve stroke outcome, we investigated the effects of metabolic endotoxemia on acute ischemic brain injury after experimental

stroke in a murine model of type 2 diabetes. We hypothesized that metabolic endotoxemia will promote LPS-induced neuroinflammation and affect the outcome after stroke.

Materials and methods

Experimental animals

All animal experiments were approved by the Juntendo University Animal Ethics Committee (No. 1176) and were in accordance with Animal Research: Reporting in Vivo Experiments (ARRIVE) reporting guidelines for the care and use of laboratory animals. We strictly followed *the National Institutes of Health Guide for the Care and Use of Laboratory Animals*.

Leptin receptor-deficient (*db/db*) mice exhibit features of type 2 diabetes.[9] We purchased 8-week-old male *db/db* mice (n = 63) and lean, phenotypically normal littermates (*db/+* mice) (n = 65) from Charles River Laboratories Japan, Inc. Mice were maintained on a 12-h light/dark cycle with *ad libitum* access to standard chow and tap water. In some animals, we used polymyxin B, a non-absorbable antibiotic, which selectively acts on Gram-negative bacteria. In the polymyxin B-treatment group, mice received 1 mg of polymyxin B (WAKO, Osaka, Japan) dissolved in 0.2 mL of distilled water once daily by oral gavage for one week. In

the non-treatment group, mice received 0.2 mL of distilled water once daily by oral gavage for one week. The treatment schedule was identical for both groups. This treatment began when mice were 11 weeks old (Figure 1(a)).

Polymyxin B plasma concentration

Plasma samples of *db/db* mice were collected 4 h after oral administration of polymyxin B. Polymyxin B standard (Hycult Biotech, PA, USA) and samples were analyzed using an enzyme-linked immunosorbent assay (ELISA). Briefly, plasma samples were added to LPS-coated plates (Hycult Biotech) and incubated with 200 μL of blocking buffer for 1 h. Subsequently, anti-polymyxin B immunoglobulin M (IgM; Hycult Biotech) was added and incubated for 1 h. Anti-mouse IgM horseradish peroxidase (Hycult Biotech) was used as a secondary antibody. Finally, 3,3',5,5'-tetramethylbenzidine (TMB) (Scy Tech, West Logan, UT, USA) and a stop solution were added to each well. Optical density values at 450 nm minus those obtained at 570 nm were analyzed.

Middle cerebral artery occlusion (MCAO)

Mice were anesthetized with 4.0% isoflurane (Abbott Japan Co., Ltd., Tokyo, Japan) and maintained with 1.0%–1.5% isoflurane in 70% N_2O and 30% O_2 using a small-animal anesthesia system. All surgical instruments were sterilized prior to surgery. Before any incision was made, the area was swabbed with ethanol. Transient cerebral focal ischemia was induced by MCAO for 60 min using an intraluminal filament technique as described previously (Figure 1(a)).[17] Briefly, the left common carotid artery and the left external carotid artery were exposed and ligated after a ventral midline neck incision. A silicon-coated nylon monofilament was inserted through the left common carotid artery into the left internal carotid artery to occlude the left MCA. After 60 min of occlusion, the monofilament was withdrawn for reperfusion. Regional cerebral blood flow (rCBF) was measured in the left temporal window on laser Doppler-flowmetry (FLOW-C1; Omegawave Inc., Tokyo, Japan) before, during, and 24 h after MCAO. We excluded mice (n = 5) in which the reduction in rCBF of the laser Doppler signal was below 60%, when compared with the preischemic state. During the procedure, a core body temperature of 37.0 ± 0.5 °C was maintained using a heating pad.

Functional outcome testing and 7-day survival rate

Neurological severity was assessed 1 h and 24 h after MCAO on a scale of 0 (normal) to 18 (maximal deficit) using the Modified Neurological Severity Score, which is a composite of motor (muscle status, abnormal movement, and balance), sensory (visual, tactile, and proprioceptive), and reflex test scores.[18] In the severity scores of injury, 1 score point is awarded for the inability to perform the test or for the lack of a tested reflex; thus, the higher the score, the more severe the injury. The 7-day survival rate for each group was determined using the Kaplan-Meier analysis.

LPS administration

In a subgroup of polymyxin B-treated *db/db* mice, LPS (*Escherichia coli* 0111: B4, 100 μg/kg; Sigma-Aldrich Co., St. Louis, MO, USA) dissolved in sterile saline or vehicle (sterile saline) was injected intraperitoneally 30 min before the induction of MCAO as previously described.[5,6]

Biochemical assays

Blood samples were collected from 12-week-old *db/+* and *db/db* mice treated with either distilled water or

polymyxin B (Figure 1(a)). Plasma glucose levels before MCAO were measured using a blood glucose meter (Johnson & Johnson, New Brunswick, NJ, USA). Plasma cytokine levels before MCAO were measured using ELISA. These measured cytokines included tumor necrosis factor-α (TNF-α) (LifeSpan BioSciences, Seattle, USA; sensitivity 15.63 pg/mL), interleukin (IL)-1β (R&D Systems, Minneapolis, MN, USA; sensitivity 2.31 pg/mL), and IL-6 (R&D Systems; sensitivity 1.6 pg/mL). Plasma LPS levels were measured before and 24 h after MCAO. Plasma samples for LPS measurements were stored in LPS-free glass tubes and heated to 70 °C for 5 min before LPS measurement. Plasma LPS concentrations were determined using a kit based on a Limulus amebocyte extract (LPS kit, Cusabio, USA).

Intestinal permeability

Intestinal permeability was measured as described previously.[8,19] Briefly, mice that had fasted for 6 h received 4,000 kDa fluorescein isothiocyanate (FITC)-dextran (440 mg/kg body weight, 100 mg/mL) dissolved in deionized water by oral gavage before or 3 h after MCAO. The mice were anesthetized 1 h after oral gavage, and a cardiac puncture was performed to collect blood. Plasma samples were diluted in equal volumes of phosphate-buffered saline (PBS; pH 7.4) and analyzed for FITC-dextran content with a

fluorescence spectrophotometer (Mithras^2 LB 943 microplate reader, Berthold Technologies, Bad Wildbad, Germany) at an excitation wavelength of 485 nm and an emission wavelength of 528 nm.

16S and 23S rRNA-targeted quantitative reverse transcription (qRT)-polymerase chain reaction (PCR)

Fecal samples were collected from 12-week-old *db/+* and *db/db* mice treated with either distilled water or polymyxin B, before and 24h after MCAO (Figure 1(a)). The composition of fecal gut microbiota was determined via 16S and 23S rRNA-targeted qRT-PCR using the Yakult Intestinal Flora-SCAN analysis system (YIF-SCAN®, Yakult Honsha Co., Ltd., Tokyo, Japan) as previously described.[20] The sequences of primers used for these analyses are listed in Supplementary Table 1.

Tissue processing

Mice were anesthetized by an intraperitoneal injection of pentobarbital (50 mg/kg) 24 h after MCAO and transcardially perfused with 20 mL ice-cold PBS to remove blood from the brain capillaries as described previously.[21] The brains turned completely white. For histological analysis, brains were subsequently perfused with 4% paraformaldehyde in PBS, which was then removed, and brains were post-fixed in the

same fixative overnight at 4 °C. Subsequently, each brain was soaked overnight in 30% sucrose in PBS. For western blot analysis and ELISA, brains were removed immediately after PBS perfusion and stored at −80 °C.

Measurement of infarct volume

For infarct quantification, forebrains were coronally sectioned into 20-µm-thick sections on a cryostat (Model CM 1900, Leica, Germany) separated by 1-mm intervals. Sections were stained with Cresyl Violet and scanned using the AxioVision software (Carl Zeiss, Jena, Germany). Image analyses were performed using the ImageJ software (National Institutes of Health; https://imagej.nih.gov/ij/). Infarct volumes and hemispheric volumes were calculated using numerical integrations of the respective areas for all sections and the distance between them. Corrected infarct volumes were calculated to compensate for the effect of brain edema using the following equation: corrected infarct volume = infarct volume – (ipsilateral hemisphere volume – contralateral hemisphere volume).[22]

Blood-brain barrier evaluation

To evaluate the permeability of the blood-brain barrier, brain sections (20-µm-thick) collected 24 h after MCAO were incubated in 3% H_2O_2 followed by blocking with 10% bovine serum albumin (Sigma-Aldrich) in PBS. Afterward, sections were incubated overnight at 4 °C with donkey anti-mouse IgG (1:300 dilution; Vector Laboratories, Burlingame, CA, USA). Immunoreactivity was visualized using the avidin-biotin complex method (Vectastain ABC kit, 1:400 dilution; Vector Laboratories). IgG was quantified for blood-brain barrier disruption using Image J.

Immunohistochemical analysis

Immunohistochemical analysis was performed on brains harvested 24 h after MCAO. Sections of forebrains (20-µm-thick) were incubated with anti-ionized calcium-binding adapter molecule antibody (Iba1, 1:500 dilution; WAKO), treated with biotinylated secondary antibody (1:300 dilution; Vector Laboratories), and subsequently processed with an avidin-biotinylated peroxidase complex (Vectastain ABC kit; 1:400 dilution; Vector Laboratories). To assess microglia/macrophage activation, the total number of Iba1-stained cells as well as the Iba1-stained area were calculated at the ischemic boundary area (0.25 mm^2) 24 h after

MCAO using ImageJ as previously described.[23]

Double immunofluorescence staining was performed by simultaneous incubation of the sections with the following primary antibodies overnight at 4 °C: anti-*Escherichia coli* LPS (1:100 dilution; Abcam) and anti-*E. coli* K99 (1:100 dilution; Lifespan, Providence, RI, USA), anti-TLR4 (1:100 dilution; Santa Cruz Biotechnology), anti-Iba1 (1:100 dilution; Abcam), anti-NeuN (neuron) (1:100 dilution; Abcam), anti-CD31 (endothelial cells) (1:25 dilution; Abcam), anti-glial fibrillary acidic protein (GFAP) (1:500 dilution; Abcam), and anti-transmembrane protein 119 (TMEM119) (1:150 dilution; Abcam). Thereafter, sections were incubated with a FITC-conjugated secondary antibody (Jackson ImmunoResearch, Baltimore, USA) for the identification of *E. coli* LPS (1:250 dilution), *E. coli* K99 (1:250 dilution), or TLR4 (1:500 dilution), and a Cy™3-conjugated secondary antibody (Jackson ImmunoResearch) for the identification of Iba1 (1:1000 dilution), NeuN (1:500 dilution), CD31 (1:500 dilution), GFAP (1:500 dilution) or TMEM119 (1:1000 dilution). Sections were covered with Vectashield mounting medium (Vector Laboratories), and immunofluorescent images were obtained using a laser-scanning microscope (model LSM780, Carl Zeiss). In immunohistochemical analyses, positively stained cells in the ischemic boundary area (0.25 mm^2) were counted in three sections from each mouse using the ZEN 2011 software (Carl Zeiss). TLR4 expression

was quantified by measuring the percentage of TLR4 immunostaining area in Iba1-, NeuN-, and CD31-positive cells, and the percentage of TMEM119-positive microglia in Iba1-positive cells was quantified using ImageJ. All immunohistochemical data were analyzed in the ipsilateral hemisphere in three coronal sections at +0.4 mm, +0.8 mm, and +1.2 mm from the bregma. Immunopositive cells were counted manually by a researcher who was blinded to the experimental conditions. The average cell number of all the sections was used as the cell number per mouse.

Western blot analysis

Mouse brain samples were obtained 24 h after reperfusion. Samples were homogenized with lysis buffer (CelLytic MT Cell Lysis Reagent; Sigma-Aldrich Co., St. Louis, MO, USA) containing a protease inhibitor cocktail (Complete Mini, EDTA-free; Roche). Homogenized samples were centrifuged at 12000 × *g* for 20 min, and pellets were discarded. Aliquots of supernatants containing 25 μg of protein were subjected to 4%–15% sodium dodecyl sulfate-polyacrylamide gel electrophoresis (SDS-PAGE) and transferred to polyvinylidene difluoride membranes (Bio-Rad Laboratories, Hercules, CA, USA). The membranes were blocked in Brockace (Dainichi-Seiyaku, Gifu, Japan) for 60 min at room temperature. Subsequently,

membranes were incubated overnight at 4 °C with antibodies against TLR4 (1:500 dilution; Santa Cruz Biotechnology, Santa Cruz, CA, USA), LPS (1:500 dilution; Abcam, Cambridge, MA, USA), and β-actin (1:5000 dilution, Abcam) followed by incubation with secondary antibodies and visualization via enhanced chemiluminescence (GE Healthcare UK, Little Chalfont, Buckinghamshire, UK).

Brain inflammatory cytokine measurement

Mouse brain samples were obtained 24 h after reperfusion. Samples were homogenized with PBS and centrifuged at 5000 × *g* for 5 min. The supernatant was collected and assayed immediately. Levels of inflammatory cytokines including TNF-α (LifeSpan BioSciences; sensitivity 15.63 pg/mL), IL-1β (R&D Systems; sensitivity 2.31 pg/mL), and IL-6 (R&D Systems; sensitivity 1.6 pg/mL) were measured using ELISA according to the manufacture's protocol.

Statistical analysis

Power estimates were calculated with the values $\alpha = 0.05$ and $\beta = 0.8$ to obtain group sizes appropriate for detecting effect sizes in the range of 30%–50% for in vivo models. Goodness-of-fit to a normal distribution

was assessed by the Shapiro-Wilk test. Data are presented as mean ± standard deviation (SD). One-way analysis of variance with Tukey's HSD *post hoc* tests was used to determine the significant differences between groups. Wilcoxon rank-sum test was used to determine the significant differences in neurological severity scores. Statistical analyses were performed using JMP 12.0.1 software (SAS Inc., Cary, NC, USA). A value of $P < 0.05$ was considered to indicate statistical significance. All experiments and measurements, including behavior outcome assessment, infarct volume measurement, and histological analysis, were performed in a blinded and randomized manner.

Results

Metabolic endotoxemia is associated with a worse stroke outcome

Male 12-week-old *db/db* mice showed higher levels of blood glucose (Figure 1(b)); inflammatory cytokines such as TNF-α, IL-1β, and IL-6 (Figure 1(c)); and body weight (Figure 1(d)) than *db/+* mice before stroke induction. We orally administered polymyxin B and measured its plasma concentrations in *db/db* mice and confirmed that polymyxin B was not absorbed from the intestine (data not shown). *Db/db* mice treated with polymyxin-B had glucose levels (Figure 1(b)) and body weight (Figure 1(d)) similar to those in untreated

db/db mice and higher than those in *db/+* mice. However, the levels of TNF-α, IL-1β, and IL-6 in polymyxin B-treated *db/db* mice were similar to those in *db/+* mice and lower than those in untreated *db/db* mice (Figure 1(c)). Furthermore, *db/db* mice showed higher plasma LPS levels than *db/+* mice or *db/db* mice treated with polymyxin B (Figure 1(e)), accompanied by an increased intestinal permeability (Figure 1(f)) reflecting metabolic endotoxemia. To evaluate changes in gut microbiota composition, we analyzed bacterial 16S and 23S rRNA in feces of *db/db* and *db/+* mice (Figure 1(g), Supplementary Figure. 1(a), and Supplementary Table 2). The fecal counts for *Atopobium* cluster, *Enterobacteriaceae*, and *Enterococcus* were higher, whereas the count for *Clostridium perfringens* was lower in *db/db* mice than in *db/+* mice. *Bifidobacterium* was undetectable in *db/db* mice. Polymyxin B administration attenuated the fecal count of *Enterobacteriaceae* in *db/db* mice. Although, the number of some bacteria differ among *db/+*, *db/db*, and polymyxin-B treated *db/db* mice, the total bacterial count was not different among these mice. This is due to the fact that the bacterial number of predominant bacteria including the *Clostridium coccoides* group, *Clostridium leptum* subgroup, *Bacteroides fragilis* group, and *Lactobacillus* that corresponds to approximately 80% to 90% of all bacteria, was not different among the groups (Supplementary Figure 2).

Subsequently, we induced transient MCAO in *db/+*, *db/db*, and polymyxin B-treated *db/db* mice.

Physiological parameters such as weight loss (Supplementary Figure 3(a)) and rCBF (Supplementary Figure 3(b)) did not differ among the groups. Plasma LPS levels (Supplementary Table 3) and intestinal permeability (Supplementary Table 4) after MCAO were higher than those before MCAO in all groups. In addition, *db/db* mice showed higher plasma LPS levels (Figure 2(a)) and intestinal permeability (Figure 2(b)) after MCAO among the groups. Differences were observed in bacterial number and detection rates in some bacteria between those before and after MCAO (Supplementary Figure 4). Particularly, the bacterial number of *Lactobacillus* was higher after MCAO than before MCAO in all groups. Furthermore, the bacterial number and detection rates of *Bifidobacterium* in *db/+* and polymyxin B-treated *db/db* mice, *Enterococcus* in *db/db* mice, and *Atopobium* cluster, *Clostridium perfringens*, and *Enterobacteriaceae* in all groups, were lower after MCAO compared to those before MCAO. However, the gut microbiota compositions after MCAO were not different among *db/+*, *db/db*, and polymyxin B-treated *db/db* mice (Figure 2(c), Supplementary Table 5 and Supplementary Figure 1(b)).

Infarct volumes (Figure 3(a)) and blood-brain barrier damage (Figure 3(b)) were greater in *db/db* mice than in *db/+* mice 24 h after MCAO. In addition, Iba1-positive microglia/macrophages in peri-infarct areas in *db/+* mice were highly ramified, whereas those in *db/db* mice exhibited a less ramified and even amoeboid

cell morphology (Figure 3(c)). The number of Iba1-positive cells and Iba1-immunoreactive areas were higher in *db/db* than in *db/+* mice in peri-infarct areas 24 h after MCAO (Figure 3(c)). To analyze Iba1-positive cells in more detail, we performed immunohistochemical analysis using TMEM119, which is a specific marker of the tissue resident microglia (Figure 3(d)). Total number of both TMEM119-positive and TMEM119-negative cells were higher in *db/db* than *db/+* mice in the peri-infarct area 24 h after MCAO (Figure 3(e)). The percentage of TMEM119-positive cells in the Iba1-positive cells was approximately 60% in both groups (Figure 3(e)). Additionally, *db/db* mice showed higher neurological severity scores 24 h after MCAO (Figure 3(f)) and a poorer 7-day survival rate (Figure 3(g)) than *db/+* mice. However, polymyxin B treatment partially reduced the infarct volumes (still increased in comparison to *db/+* mice) (Figure 3(a)) and blood-brain barrier damage (Figure 3(b)), as well as changed the morphology of Iba1-positive cells to a ramified phenotype (Figure 3(c), decreased Iba1-positive cell number and areas (Figure 3(c)), and improved neurological function 24 h after MCAO (Figure 3(f)) and 7-day survival (Figure 3(g)) in *db/db* mice.

Because polymyxin B treatment attenuated the circulating LPS levels and ameliorated the stroke outcome in *db/db* mice, we examined the direct impact of LPS on stroke outcome in *db/db* mice. In polymyxin B-

treated *db/db* mice, intraperitoneal LPS administration before MCAO increased the infarct volume (Figure 3(h)) and number of Iba1-positive cells and Iba1-immunoreactive areas in the peri-infarct area (Figure 3(i)), as well as the neurological severity score (Figure3(j)), 24 h after MCAO.

In the normoglycemic control *db/+* mice, infarct volume (Figure 3(a)) and stroke outcomes such as neurological severity score (Figure 3(f)) and survival rate after MCAO (Figure 3(g)) were comparable to those in C57BL/6 mice, which has been reported in our previous study.[17] Oral gavage of polymyxin B did not show any effects on plasma LPS levels (Supplementary Figure 5(a)), intestinal permeability (Supplementary Figure 5(b), infarct volumes 24 h after MCAO (Supplementary Figure 5(c)) and neurological functions 1 h and 24 h after MCAO (Supplementary Figure 5(d)) in *db/+* mice. Additionally, the bacterial counts did not change between *db/+* and polymyxin B-treated *db/+* mice 24 h after MCAO (Supplementary Figure 5(e)).

LPS and neuroinflammation in the ischemic brain

Since we found that metabolic endotoxemia was associated with worse stroke outcome, we analyzed the presence of LPS in the brain 24 h after ischemia. Western blot analysis revealed that LPS levels were higher

in the ischemic hemispheres of *db/db* mice compared to those of *db/+* mice; LPS levels were attenuated by polymyxin B treatment in *db/db* mice (Figure 4(a)). In all groups, LPS was not detected in the contralateral, non-ischemic hemispheres (Supplementary Figure 6(a)). Next, we examined the expression levels of TLR4, an LPS receptor, and inflammatory cytokines in the ischemic brain. Expression levels of TLR4 (Figure 4(b)), TNF-α, IL-1β, and IL-6 (Figure 4(c)) were higher in *db/db* mice than in *db/+* mice, but lower in polymyxin B-treated *db/db* mice than in untreated *db/db* mice. The expression levels of TLR4 and these inflammatory cytokines in the contralateral hemispheres did not change among these groups (Supplementary Figure 6(b) and (c)).

Localization of LPS, E. coli K99 pili protein, and TLR4 in the ischemic brain

We examined the localization of LPS and *E. coli* (which belongs to the *Enterobacteriaceae* family) K99 pili protein in the brain 24 h after ischemia. The immunohistochemical analysis demonstrated that LPS (Figure 5(a)) and *E. coli* K99 pili protein (Figure 5(b)) were localized in the peri-infarct area in Iba1-positive microglia/macrophages, neurons, and endothelial cells, but not in astrocytes. High magnification images showed that LPS (Figure 5(a)) and *E. coli* K99 pili protein (Figure 5(b)) were adherent on the surface of

Iba1-positive microglia/macrophages, neurons, and endothelial cells. Neither LPS nor *E. coli* K99 pili protein was detected in the contralateral hemispheres (data not shown). We also observed in the peri-infarct area, TLR4 immunoreactivity in Iba1-positive microglia/macrophages, neurons, and endothelial cells, but not in astrocytes (Figure 5(c)). The percentages of TLR4-immunoreactive areas in these cells were higher in *db/db* mice compared to *db/+* mice and polymyxin B-treated *db/db* mice (Figure 5(d)).

Discussion

The present study demonstrates that metabolic endotoxemia is negatively associated with stroke outcome. Increased intestinal permeability and circulating LPS levels were associated with increased levels of LPS, TLR4, and inflammatory cytokines in the ischemic brain in diabetic mice (Figure 6). Moreover, gut microbiota modulation with a non-absorbable antibiotic polymyxin B attenuated LPS levels in the circulation, thereby in the ischemic brain and improved the stroke outcome. Notably, LPS administration attenuated the positive effects of gut microbiota modulation with the antibiotic on stroke outcomes. Additionally, polymyxin B treatment had no effect on stroke outcomes in control mice, in which, circulating LPS levels were much lower than in diabetic mice. These findings suggest an association between

metabolic endotoxemia and the pathophysiology of acute ischemic brain injury via the Gram-negative bacterial toxin LPS in diabetic mice.

In the present study, *db/db* mice showed enrichment of fecal *Enterobacteriaceae*. *Enterobacteriaceae* are a large family of Gram-negative bacteria that includes opportunistic pathogens such as *E. coli*, *Klebsiella*, and *Salmonella*. Consistent with the results of our study, a previous study in *db/db* mice also showed an increase in *Proteobacteria* (this phylum contains *Enterobacteriaceae*).[24] An increase in the number of *Proteobacteria* is observed during gut dysbiosis in several diseases including inflammatory bowel disease, colorectal cancer, metabolic syndrome, and type 2 diabetes.[25] In addition, a previous clinical study showed that acute stroke patients had a more abundant presence of *Enterobacter* (which belongs to the *Enterobacteriaceae* family).[26] However, dysbiosis with expansion of the *Burkholderiaceae* family, which belongs to the *Proteobacteria*, is associated with neuroprotective effects on ischemic cerebral injury in mice.[27]

Polymyxin B is one of the primary classes of antibiotics with activity against most Gram-negative bacteria.[28] In our bacterial analysis, Gram-negative bacteria included the *Bacteroides fragilis* group, *Prevotella*, *Enterobacteriaceae*, and *Pseudomonas*. However, *Prevotella* and *Pseudomonas* were

undetectable in all groups. Polymyxin B attenuated *Enterobacteriaceae*. However, polymyxin B had no effects on the bacterial counts of *Bacteroides fragilis*, known to be resistant to this antibiotic.[29] We showed that increased fecal levels of *Enterobacteriaceae* were associated with increases in circulating LPS levels concurrent with increased intestinal permeability before stroke induction. Emerging evidence has revealed that gut microbiota has potent effects on intestinal permeability. The proliferation of *Enterobacteriaceae* leads to an increase in luminal LPS content in the gut, which results in changes in tight junction proteins and an increase in intestinal permeability through TLR4-induced inflammation.[30] The substantial changes in expression/distribution of tight junction proteins with enhanced intestinal permeability have been shown to lead to an abnormal leakage of bacterial LPS into the circulatory system in *db/db* mice.[9] We also found that higher plasma LPS levels were associated with increasing inflammatory cytokine levels, while gut microbiota modulation reduced circulating LPS levels and inflammatory signaling. These findings are consistent with a previous report investigating endotoxemia and systemic inflammation using *db/db* mice.[9] Furthermore, our study found that *Bifidobacterium* was undetectable in feces of *db/db* mice before stroke induction. Decreased *Bifidobacterium* levels have been implicated in intestinal barrier dysfunction and LPS translocation.[31,32] Therefore, the reduction in *Bifidobacterium* may also have increased the levels of

circulating LPS in *db/db* mice in our study. Additionally, our study showed that the number of *Clostridium perfringens* in *db/db* mice was lower than that in *db/+* mice. This finding is in line with a previous study, which showed a lower amount of *Clostridium perfringens* in obese subjects compared to normal-weight people.[33] Thus, a decrease in the number of *Clostridium perfringens* may be associated with an obese phenotype. However, these Gram-positive bacteria were not affected by polymyxin B treatment in *db/db* mice, suggesting *Clostridium perfringens* may not have contributed to endotoxemia before stroke induction in these mice.

Lately, special focus has been placed on the gut-brain axis in ischemic stroke pathophysiology. Gut microbiota have been implicated in ischemic brain injury after stroke via the regulation of intestinal T cells.[27,34] Additionally, stroke causes specific changes in gut microbiota, which in turn contributes to stroke outcomes.[34,35,36] Stroke also promotes the translocation and dissemination of bacteria from host gut microbiota as a mechanism leading to post-stroke infection.[19] Recently, Gram-negative bacteria-derived LPS has been implicated in the neuropathology of the human brain. For example, LPS and the K99 pili protein of Gram-negative *E. coli* bacteria were detected at higher levels in brains of patients with Alzheimer's disease compared to controls and were colocalized with amyloid β in amyloid plaques and

around vessels.[37] However, the origin of these bacterial molecules in the brain is currently not well understood.

In the current study, we determined the presence of LPS and *E. coli* K99 pili protein in the ischemic brain 24 h after cerebral ischemia. Lipopolysaccharide levels in the ischemic brain were attenuated by oral gavage of the non-absorbable antibiotic, polymyxin B in *db/db* mice. These findings were associated with suppression of fecal *Enterobacteriaceae* counts, intestinal permeability, and circulating LPS levels before stroke induction. We also found that intestinal permeability was further enhanced after MCAO in all group mice. These findings were in line with a previous study investigating the intestinal permeability in mice subjected to MCAO.[19] Importantly, our study showed that *db/db* mice had the most prominent increase of plasma LPS levels and intestinal permeability after MCAO among groups. Our study also showed that stroke induced certain changes in gut microbiota, particularly an increase in *Lactobacillus,* which is in line with a previous study.[36] Additionally, some non-predominant bacteria were reduced or undetectable after MCAO. Reduction in species diversity is a key feature of dysbiosis after stroke.[34] However, the gut microbiota compositions after MCAO were not different among *db/+*, *db/db*, and polymyxin B-treated *db/db* mice. Therefore, our findings suggest that stroke has a greater impact on gut microbiota composition

than the phenotypes such as type 2 diabetes.

Toll-like receptor 4 plays an important role in post-stroke inflammation and contributes to the progression of brain damage, whereas genetic deletion of TLR4 significantly reduces the infarct volume.[38] Damage-associated molecular patterns released from injured neurons such as high mobility group box 1[39] and peroxiredoxin family proteins[40] activate TLR4 in the brain after cerebral ischemia. Among the members of the TLR family, TLR4 is mainly involved in LPS-mediated inflammatory responses.[1] In the present study, TLR4 and inflammatory cytokine levels in the ischemic brain were significantly higher in *db/db* compared to *db/+* mice. These findings were associated with LPS levels in ischemic brains; the reduction in LPS levels in polymyxin B-treated *db/db* mice decreased TLR4 and inflammatory cytokine levels. We also found that *db/db* mice showed higher levels of plasma inflammatory cytokines compared with *db/+* and polymyxin B-treated *db/db* mice. Therefore, although ischemic injury increases TLR4 activation,[39,40] it is also possible that influx of LPS, as well as extravasation of plasma inflammatory cytokines into the ischemic brain, also contribute to neuroinflammation.

In the peri-infarct area, we found that LPS and *E. coli* K99 pili protein were adherent on the surface of Iba1-positive microglia/macrophages, endothelial cells, and neurons, but not in astrocytes. Furthermore,

Iba1-positive microglia/macrophages, endothelial cells, and neurons, except astrocytes expressed TLR4. Immunoreactive areas of TLR4 in these cells were higher in *db/db* mice compared to *db/+* and polymyxin B-treated *db/db* mice, suggesting TLR4 activation was pronounced in *db/db* mice. Among the major non-neuronal cell types in the brain, microglia expressed high levels of TLR4, whereas astrocytes expressed none.[41] Furthermore, microglia are the only glial cells that bind LPS.[41] These findings suggest that microglia/macrophages contribute to LPS-induced neuroinflammation. The question of TLR4 expression in astrocytes has not been undeniably clarified, since in different studies TLR4 was either absent[41,42] or present.[43] These inconsistencies in the reported expression patterns may be related to differences in the experimental paradigms and immunoprobes used. Endothelial cells also express TLR4[44] and produce cytokines in response to LPS stimulation.[45] Additionally, LPS has been reported to induce inflammatory cytokine production in neurons via TLR4 activation.[46]

Our study showed that Iba1-positive cells in *db/+* mice were characterized by a highly ramified shape, whereas those in *db/db* mice showed a less ramified or amoeboid cell morphology, reflecting their activation status.[47] The origin of cells identified by Iba1 could either be activated brain-resident microglia or macrophages derived from circulating monocytes.[47] The TMEM119 is a recently identified highly

specific cell-surface marker of microglia that is not expressed by macrophages or other immune or neural cell types.[48] Our study showed that approximately 60% of Iba1-positive cells expressed TMEM119 in both *db/+* and *db/db* mice. This is in line with a pathological study of human brains showing that 43% of Iba1-positive cells at the edge of acute ischemic lesions expressed TMEM119.[49] Altogether, these findings suggest that Iba1-positive cells consist in part of resident microglia, and in part of infiltrating macrophages in per-infarct areas of acute cerebral ischemia.

Although systemic LPS administration has been shown to disrupt the blood-brain barrier,[50] we did not see significant differences in IgG staining in the contralateral, non-ischemic hemispheres among *db/+*, *db/db,* and polymyxin B-treated *db/db* mice. Indeed, LPS was not detected and levels of TLR4 and inflammatory cytokines were not different in the non-ischemic hemispheres in all these mice. This might be explained by differences in experimental models (systemic LPS administration vs. metabolic endotoxemia), which may result in different effects on the blood-brain barrier.

Interestingly, LPS preconditioning provides neuroprotective effects via several mechanisms including proinflammatory cytokine production. Induction of TNF-α by LPS administration before stroke causes ischemic tolerance by suppressing the TNF-α response to cerebral ischemic injury.[51] Furthermore, LPS pre-

treatment reduces *N*-methyl-D-aspartate-mediated cerebral injury by inducing nitric oxide and cGMP.[52] Thus, LPS can be neuroprotective when it is administered under optimal conditions (dose and timing). However, our study indicated that chronic exposure to LPS may be deleterious by increasing neuroinflammation after stroke.

Among the cardiovascular risk factors, type 2 diabetes is considerably associated with poor functional outcomes after stroke.[14] Yet, controlling post-stroke hyperglycemia has no effect on the outcome in experimental animal models[15] or stroke patients.[16] In the present study, we demonstrated that the reduction in circulating LPS levels was associated with an attenuation of inflammatory cytokine production, as well as with improvements in neurological functions and survival after stroke, without influencing plasma glucose levels in a mouse model of type 2 diabetes. Although our study demonstrated that polymyxin B was effective to reduce the bacterial counts of *Enterobacteriaceae* and thereby decrease circulating LPS levels, antibiotic treatment may not be suitable for the clinical setting due to potential undesirable side effects associated with antibiotic treatment and the risk of emergence of antibiotic-resistant bacteria. Experimental studies have shown that supplementation of *Bifidobacterium*[31] or oligofructose[32] decreases plasma LPS levels. Thus, the administration of pro- or prebiotics may be a potential treatment option to

improve stroke outcomes by preventing LPS translocation in patients with type 2 diabetes.

Although interspecies differences should always be considered, the murine gut has successfully been used as a model to investigate the role of gut microbiota in complex human disorders, including post-stroke infections, obesity, and diabetes.[8,19]

The present study had some limitations. First, although we used sterile techniques, LPS could have contaminated tissue samples. However, LPS levels were consistently higher in *db/db* compared to *db/+* and polymyxin B-treated *db/db* mice, despite using the same techniques in all groups. In addition, LPS was not detected in non-ischemic hemispheres. Second, the effects of other bacteria, not included in our microbiota analysis, need to be further investigated. However, the rRNA-targeted qRT-PCR used in this study enables high-resolution quantification of targeted bacterial populations including potentially pathogenic bacteria which might not be quantified efficiently, by either routine DNA-based PCR or next-generation sequencing methods due to their low sensitivity.[53,54] Third, we focused on LPS in the present study, but further studies are needed to examine the potential importance of other bacteria-derived molecules such as peptidoglycan in stroke pathophysiology. Additionally, as gut microbiota contributes to ischemic cerebral injury by regulating peripheral immune cells,[27,34] analyzing the impact of gut dysbiosis and polymyxin B treatment

on peripheral immune cells is crucial. Fourth, since parameters were measured post-stroke and correlated with the size of the lesion, they did not address the direct role of endotoxemia. Experiments with TLR4 knock-out mice would provide more details about the interactions between endotoxemia and neuroinflammation. Additionally, our study showed that *db/db* mice had greater ischemic damage compared to *db/+* mice 24 h after MCAO. To elucidate how the infarct develops over time, further investigations are needed at earlier time points. Finally, our results are limited to young male mice and may not be applicable to old or female mice. In addition, the 12-week-old *db/db* mice used in the current study had extremely high glucose levels, which could be responsible for the poor survival rate after stroke, and this limited the ability to conduct long-term studies on the effect of polymyxin B or the effects of polymyxin B administration after stroke. Particularly, it would be of interest to examine whether LPS that remains in the brain, contributes to poststroke cognitive decline in a similar manner to Alzheimer's disease.[37] In this regard, a milder diabetic model such as high-fat diet fed-mice would be useful in future research.

In conclusion, our study suggests that metabolic endotoxemia is associated with neuroinflammation after transient focal cerebral ischemia in type 2 diabetes. Targeting metabolic endotoxemia might be a novel potential therapeutic strategy to improve stroke outcomes.

Funding

This project was funded by the JSPS KAKENHI grant no. JP15K07439.

Authors' contributions

NK, KY, TK, RT, TU, YY, NH: Conception and experimental design; NK, KY, TK, YU, NM, MT, HS, TI, KN, SM, TT, HT, TA: Experimental work; NK, KY: Interpretation of data and writing of manuscript. All authors discussed the results and provided input regarding the manuscript. All the authors have approved the final version of the manuscript.

Declaration of conflicting interests

The Authors declare that there are no conflict of interest.

Supplementary material

Supplementary material for this paper can be found at the journal website:

http://journals.sagepub.com/home/jcb

References

1. Kawai T and Akira S. The role of pattern-recognition receptors in innate immunity: update on Toll-like receptors. *Nat Immunol* 2010; 11: 373–384.

2. Macrez R, Ali C, Toutirais O, et al. Stroke and the immune system: from pathophysiology to new therapeutic strategies. *Lancet Neurol* 2011; 10: 471–480.

3. Wiedermann CJ, Kiechl S, Dunzendorfer S, et al. Association of endotoxemia with carotid atherosclerosis and cardiovascular disease: prospective results from the Bruneck Study. *J Am Coll Cardiol* 1999; 34: 1975–1981.

4. Klimiec E, Pera J, Chrzanowska-Wasko J, et al. Plasma endotoxin activity rises during ischemic stroke and is associated with worse short-term outcome. *J Neuroimmunol* 2016; 297: 76–80.

5. McColl BW, Rothwell NJ and Allan SM. Systemic inflammatory stimulus potentiates the acute phase and CXC chemokine responses to experimental stroke and exacerbates brain damage via interleukin-1- and neutrophil-dependent mechanisms. *J Neurosci* 2007; 27: 4403–4412.

6. Doll DN, Hu H, Sun J, et al. Mitochondrial crisis in cerebrovascular endothelial cells opens the blood-brain barrier. *Stroke* 2015; 46: 1681–1689.

7. Odenwald MA and Turner JR. The intestinal epithelial barrier: a therapeutic target? *Nat Rev Gastroenterol Hepatol* 2017; 14: 9–21.

8. Cani PD, Bibiloni R, Knauf C, et al. Changes in gut microbiota control metabolic endotoxemia-induced inflammation in high-fat diet-induced obesity and diabetes in mice. *Diabetes* 2008; 57: 1470-1481.

9. Brun P, Castagliuolo I, Di Leo V, et al. Increased intestinal permeability in obese mice: new evidence in the pathogenesis of nonalcoholic steatohepatitis. *Am J Physiol Gastrointest Liver Physiol* 2007; 292: G518–G525.

10. Creely SJ, McTernan PG, Kusminski CM, et al. Lipopolysaccharide activates an innate immune system response in human adipose tissue in obesity and type 2 diabetes. *Am J Physiol Endocrinol Metab* 2007; 292: E740–E747.

11. Sato J, Kanazawa A, Ikeda F, et al. Gut dysbiosis and detection of "live gut bacteria" in blood of Japanese patients with type 2 diabetes. *Diabetes Care* 2014; 37: 2343–2350.

12. Urabe T, Watada H, Okuma Y, et al. Prevalence of abnormal glucose metabolism and insulin resistance among subtypes of ischemic stroke in Japanese patients. *Stroke* 2009; 40: 1289–1295.

13. Tureyen K, Bowen K, Liang J, et al. Exacerbated brain damage, edema and inflammation in type-2 diabetic mice subjected to focal ischemia. *J Neurochem* 2011; 116: 499–507.

14. Tanaka R, Ueno Y, Miyamoto N, et al. Impact of diabetes and prediabetes on the short-term prognosis in patients with acute ischemic stroke. *J Neurol Sci* 2013; 332: 45–50.

15. MacDougall NJ and Muir KW. Hyperglycaemia and infarct size in animal models of middle cerebral artery occlusion: systematic review and meta-analysis. *J Cereb Blood Flow Metab* 2011; 31: 807–818.

16. Johnston KC, Bruno A, Pauls Q, et al. Intensive vs Standard Treatment of Hyperglycemia and Functional Outcome in Patients With Acute Ischemic Stroke: The SHINE Randomized Clinical Trial. *JAMA* 2019; 322: 326-335.

17. Kuroki T, Tanaka R, Shimada Y, et al. Exendin-4 inhibits matrix metalloproteinase-9 activation and reduces infarct growth after focal cerebral ischemia in hyperglycemic mice. *Stroke* 2016; 47: 1328–1335.

18. Chen J, Li Y, Wang L, et al. Therapeutic benefit of intravenous administration of bone marrow stromal cells after cerebral ischemia in rats. *Stroke* 2001; 32: 1005–1011.

19. Stanley D, Mason LJ, Mackin KE, et al. Translocation and dissemination of commensal bacteria in post-stroke infection. *Nat Med* 2016; 22: 1277-1284.

20. Yamashiro K, Tanaka R, Urabe T, et al. Gut dysbiosis is associated with metabolism and systemic inflammation in patients with ischemic stroke. *PLoS One* 2017; 12: e0171521.

21. Gregersen R, Lambertsen K, Finsen B. Microglia and macrophages are the major source of tumor necrosis factor in permanent middle cerebral artery occlusion in mice. *J Cereb Blood Flow Metab* 2000; 20: 53-65.

22. Bastide M, Bordet R, Pu Q, et al. Relationship between inward rectifier potassium current impairment and brain injury after cerebral ischemia/reperfusion. *J Cereb Blood Flow Metab* 1999; 19: 1309-1315.

23. Tanaka M, Ishihara Y, Mizuno S, et al. Progression of vasogenic edema induced by activated microglia under permanent middle cerebral artery occlusion. *Biochem Biophys Res Commun* 2018; 496: 582-587.

24. Geurts L, Lazarevic V, Derrien M, et al. Altered gut microbiota and endocannabinoid system tone in obese and diabetic leptin-resistant mice: impact on apelin regulation in adipose tissue. *Front*

Microbiol 2011; 2: 149.

25. Shin NR, Whon TW and Bae JW. Proteobacteria: microbial signature of dysbiosis in gut microbiota. *Trends Biotechnol* 2015; 33: 496–503.

26. Yin J, Liao SX, He Y, et al. Dysbiosis of gut microbiota with reduced trimethylamine-N-oxide level in patients with large-artery atherosclerotic stroke or transient ischemic attack. *J Am Heart Assoc* 2015; 4: e002699.

27. Benakis C, Brea D, Caballero S, et al. Commensal microbiota affects ischemic stroke outcome by regulating intestinal γδ T cells. *Nat Med* 2016; 22: 516-523.

28. Poirel L, Jayol A and Nordmann P. Polymyxins: antibacterial activity, susceptibility testing, and resistance mechanisms encoded by plasmids or chromosomes. *Clin Microbiol Rev* 2017; 30: 557-596.

29. Kislak JW. The susceptibility of *Bacteroides fragilis* to 24 antibiotics. *J Infect Dis* 1972; 125: 295-299.

30. Kim KA, Gu W, Lee IA, et al. High fat diet-induced gut microbiota exacerbates inflammation and obesity in mice via the TLR4 signaling pathway. *PLoS One* 2012; 7: e47713.

31. Wang Z, Xiao G, Yao Y, et al. The role of bifidobacteria in gut barrier function after thermal injury in rats. *J Trauma* 2006; 61: 650–657.

32. Cani PD, Neyrinck AM, Fava F, et al. Selective increases of bifidobacteria in gut microflora improve high-fat-diet-induced diabetes in mice through a mechanism associated with endotoxaemia. *Diabetologia* 2007; 50: 2374–2383.

33. Zuo HJ, Xie ZM, Zhang WW, et al. Gut bacteria alteration in obese people and its relationship with gene polymorphism. *World J Gastroenterol* 2011; 17: 1076-1081.

34. Singh V, Roth S, Llovera G, et al. Microbiota dysbiosis controls the neuroinflammatory response after stroke. *J Neurosci* 2016;36: 7428–7440.

35. Houlden A, Goldrick M, Brough D, et al. Brain injury induces specific changes in the caecal microbiota of mice via altered autonomic activity and mucoprotein production. *Brain Behav Immun* 2016; 57: 10-20.

36. Stanley D, Moore RJ and Wong CHY. An insight into intestinal mucosal microbiota disruption after stroke. *Sci Rep* 2018; 8: 568.

37. Zhan X, Stamova B, Jin LW, et al. Gram-negative bacterial molecules associate with Alzheimer

disease pathology. *Neurology* 2016; 87: 2324–2332.

38. Caso JR, Pradillo JM, Hurtado O, et al. Toll-like receptor 4 is involved in brain damage and inflammation after experimental stroke. *Circulation* 2007; 115: 1599–1608.

39. Qiu J, Nishimura M, Wang Y, et al. Early release of HMGB-1 from neurons after the onset of brain ischemia. *J Cereb Blood Flow Metab* 2008; 28: 927–938.

40. Shichita T, Hasegawa E, Kimura A, et al. Peroxiredoxin family proteins are key initiators of post-ischemic inflammation in the brain. *Nat Med* 2012; 18: 911–917.

41. Lehnardt S, Lachance C, Patrizi S, et al. The toll-like receptor TLR4 is necessary for lipopolysaccharide-induced oligodendrocyte injury in the CNS. *J Neurosci* 2002; 22: 2478-2486.

42. Lehnardt S, Massillon L, Follett P, et al. Activation of innate immunity in the CNS triggers neurodegeneration through a Toll-like receptor 4-dependent pathway. *Proc Natl Acad Sci USA* 2003; 100: 8514–8519.

43. Gorina R, Font-Nieves M, Márquez-Kisinousky L, et al. Astrocyte TLR4 activation induces a proinflammatory environment through the interplay between MyD88-dependent NFκB signaling, MAPK, and Jak1/Stat1 pathways. *Glia* 2011; 59: 242-255.

44. Shih RH and Yang CM. Induction of heme oxygenase-1 attenuates lipopolysaccharide-induced cyclooxygenase-2 expression in mouse brain endothelial cells. *J Neuroinflammation* 2010; 7: 86.

45. Verma S, Nakaoke R, Dohgu S, et al. Release of cytokines by brain endothelial cells: a polarized response to lipopolysaccharide. *Brain Behav Immun* 2006; 20: 449–455.

46. Leow-Dyke S, Allen C, Denes A, et al. Neuronal Toll-like receptor 4 signaling induces brain endothelial activation and neutrophil transmigration in vitro. *J Neuroinflammation* 2012; 9: 230.

47. Kettenmann H, Hanisch UK, Noda M, et al. Physiology of microglia. *Physiol Rev* 2011; 91: 461–553.

48. Bennett ML, Bennett FC, Liddelow SA, et al. New tools for studying microglia in the mouse and human CNS. *Proc Natl Acad Sci USA* 2016; 113: E1738-1746.

49. Zrzavy T, Machado-Santos J, Christine S, et al. Dominant role of microglial and macrophage innate immune responses in human ischemic infarcts. *Brain Pathol* 2018; 28: 791-805.

50. Banks WA and Erickson MA. The blood-brain barrier and immune function and dysfunction. *Neurobiol Dis* 2010; 37: 26–32.

51. Rosenzweig HL, Minami M, Lessov NS, et al. Endotoxin preconditioning protects against the

cytotoxic effects of TNFalpha after stroke: a novel role for TNFalpha in LPS-ischemic tolerance. *J Cereb Blood Flow Metab* 2007; 27: 1663-1674.

52. Orio M, Kunz A, Kawano T, et al. Lipopolysaccharide induces early tolerance to excitotoxicity via nitric oxide and cGMP. *Stroke* 2007; 38: 2812-2817.

53. Matsuda K, Tsuji H, Asahara T, et al. Sensitive quantitative detection of commensal bacteria by rRNA-targeted reverse transcription-PCR. *Appl Environ Microbiol* 2007; 73: 32–39.

54. Matsuda K, Tsuji H, Asahara T, et al. Establishment of an analytical system for the human fecal microbiota, based on reverse transcription-quantitative PCR targeting of multicopy rRNA molecules. *Appl Environ Microbiol* 2009; 75: 1961–1969.

Figure legends

Figure 1. Biological parameters of *db/+*, *db/db,* and polymyxin B (PL-B)-treated *db/db* mice measured prior to stroke induction with middle cerebral artery occlusion (MCAO). (a) Experimental design. (b) Plasma glucose levels (n = 5 per group). (c) Plasma levels of tumor necrosis factor (TNF)-α, interleukin (IL)-1β, and IL-6 (n = 5 per group). (d) Body weight (n = 6 per group). (e) Plasma lipopolysaccharide (LPS) levels (n = 6–9 per group). (f) Intestinal permeability assessed by quantitative analysis of fluorescein isothiocyanate (FITC)-dextran translocation (n = 5–6 per group). (g) Fecal bacterial counts analyzed by rRNA-targeted quantitative reverse transcription PCR (n = 5 per group). Bacterial counts below the threshold of detection were not plotted. Data are shown as mean ± SD. $*P < 0.05$, $**P < 0.01$, and $***P < 0.001$.

Figure 2. Biological parameters of *db/+*, *db/db,* and polymyxin B (PL-B)-treated *db/db* mice measured after stroke induction via middle cerebral artery occlusion (MCAO). (a) Plasma LPS levels after MCAO (n = 6–9 per group) (b) Intestinal permeability after MCAO (n = 5 per group). (c) Fecal bacterial counts after MCAO analyzed by rRNA-targeted quantitative reverse transcription PCR (n = 5 per group). Bacterial

counts below the threshold of detection were not plotted. Data are shown as mean ± SD. *$P < 0.05$, **$P < 0.01$, and ***$P < 0.001$.

Figure 3. Stroke outcomes in *db/+*, *db/db,* and polymyxin B (PL-B)-treated *db/db* mice. (a) Representative images of Cresyl Violet-stained brain sections (left) and quantification of infarct volumes (right) 24 h after middle cerebral artery occlusion (MCAO). Total hemispheric infarct volumes were corrected for edema (n = 8 per group). Scale bars = 1 mm. (b) Representative images (left) and quantification (right) of blood-brain barrier damage assessed by IgG immunoreactivity 24 h after MCAO (n = 5 per group). Scale bars = 1 mm. (c) Representative images of Iba1-positive cells, cell count of Iba1-positive cells, and percentage of Iba1-positive area in the peri-infarct area 24 h after MCAO (n = 4–6 per group). Scale bars = 20 μm. Data are shown as mean ± SD. (d) Double-immunofluorescence of Iba1 and anti-transmembrane protein 119 (TMEM119) in the peri-infarct area 24 h after MCAO in *db/+* and *db/db* mice. Scale bars = 20 μm. (e) Total number of TMEM119-positive cells and TMEM119-negative cells in Iba1-positive cells, and percentage of TMEM119-positive cells in Iba1-positive cells in the peri-infarct area 24 h after MCAO in *db/+* and *db/db* mice (n = 5 per group). (f) Modified neurological severity scores (NSS) 1 h and 24 h after

MCAO (n = 8 per group). Data are shown as median and interquartile range. (g) Seven-day survival after MCAO (n = 8–10 per group). Kaplan-Meier curve followed by the log rank test. (h) Infarct volumes 24 h after MCAO in polymyxin B-treated *db/db* mice with and without intraperitoneal lipopolysaccharide (LPS) administration. Total hemispheric infarct volumes were corrected for edema (n = 5 per group). (i) Cell count of Iba1-positive cells and percentage of Iba1-positive area in the peri-infarct area 24 h after MCAO in polymyxin B-treated *db/db* mice with and without intraperitoneal LPS administration. (n = 5 per group). Data are shown as mean ± SD. (j) Modified NSS 1 h and 24 h after MCAO in polymyxin B-treated *db/db* mice with and without intraperitoneal LPS administration (n = 5 per group). Data are shown as median and interquartile range. **P* < 0.05, ***P* < 0.01, and ****P* < 0.001.

Figure 4. Lipopolysaccharide (LPS), toll-like receptor (TLR) 4, and inflammatory cytokines in the ischemic hemispheres of *db/+*, *db/db,* and polymyxin B (PL-B)-treated *db/db* mice. Western blot analyses of (a) LPS and (b) TLR4 expression. (c) Enzyme-linked immunoassay results for tumor necrosis factor (TNF)-α, interleukin (IL)-1β, and IL-6. All data were analyzed in mice sacrificed 24 h after middle cerebral

artery occlusion (n = 5–10 per group). Data are shown as mean ± SD. *$P < 0.05$, **$P < 0.01$, and ***$P < 0.001$.

Figure 5. Cellular localization of lipopolysaccharide (LPS), *E. coli* K99 and toll-like receptor 4 (TLR4) in the peri-infarct areas of ischemic brain. Double-immunofluorescence of (a) LPS, (b) *E. coli* K99, and (c) TLR4 in microglia/macrophages (Iba1), neurons (NeuN), endothelial cells (CD31), and astrocytes (GFAP) in the peri-infarct area 24 h after transient middle cerebral artery occlusion in *db/db* mice. High magnification images show that (a) LPS and (b) *E. coli* K99 were adherent on the surface of microglia/macrophages, neurons and endothelial cells (arrows). (c) TLR4 was colocalized with Iba1, NeuN and CD31 (arrows). Scale bars = 20 μm. A red square in the brain illustration shows the region of analysis. (d) The percentages of TLR4-immunoreactive areas in Iba1, NeuN, and CD31-positive cells in *db/+*, *db/db*, and polymyxin B (PL-B)-treated *db/db* mice (n = 6 per group). Data are shown as mean ± SD. **$P < 0.01$ and ***$P < 0.001$.

Figure 6. Proposed mechanism of ischemic brain injury induced by metabolic endotoxemia. Gut dysbiosis in type 2 diabetes causes increased intestinal permeability and the translocation of microbiota-derived lipopolysaccharide (LPS) into the circulatory system. Disruption of the blood-brain barrier after cerebral ischemia allows an influx of LPS into brain parenchyma, where the induction of toll-like receptor 4 (TLR4), and inflammatory cytokines exacerbate ischemic brain injury.

Original Article

Metabolic endotoxemia promotes neuroinflammation after focal cerebral ischemia

Naohide Kurita[1], Kazuo Yamashiro[1], Takuma Kuroki[1], Ryota Tanaka[2], Takao Urabe[3], Yuji Ueno[1], Nobukazu Miyamoto[1], Masashi Takanashi[1], Hideki Shimura[3], Toshiki Inaba[3], Yuichiro Yamashiro[4], Koji Nomoto[4,5], Satoshi Matsumoto[4,6], Takuya Takahashi[4,7], Hirokazu Tsuji[4,6], Takashi Asahara[4,6] and Nobutaka Hattori[1]

[1]Department of Neurology, Juntendo University School of Medicine, Tokyo, Japan

[2]Division of Neurology, Department of Internal Medicine, Jichi Medical University, Tochigi Japan

[3]Department of Neurology, Juntendo University Urayasu Hospital, Chiba, Japan

[4]Probiotics Research Laboratory, Juntendo University Graduate School of Medicine, Tokyo, Japan

[5]Laboratory of Animal Symbiotic Microorganisms, Department of Molecular Biology, Faculty of Life Science, Tokyo University of Agriculture, Tokyo, Japan

[6]Yakult Central Institute, Tokyo, Japan

[7]Yakult Honsha European Research Center for Microbiology ESV, Gent, Belgium

Corresponding author: Kazuo Yamashiro, MD

Department of Neurology, Juntendo University School of Medicine

2-1-1 Hongo, Bunkyo-ku, Tokyo 113-8421, Japan

Tel: +81 3 3813 3111

Email: kazuo-y@juntendo.ac.jp

Running headline: Metabolic endotoxemia and stroke

Abstract

Lipopolysaccharide (LPS) is a major component of the outer membrane of Gram-negative bacteria and a potent inflammatory stimulus for the innate immune response via toll-like receptor (TLR) 4 activation. Type 2 diabetes is associated with changes in gut microbiota and impaired intestinal barrier functions, leading to translocation of microbiota-derived LPS into the circulatory system, a condition referred to as metabolic endotoxemia. We investigated the effects of metabolic endotoxemia after experimental stroke with transient middle cerebral artery occlusion (MCAO) in a murine model of type 2 diabetes (*db/db*) and phenotypically normal littermates (*db/+*). Compared to *db/+* mice, *db/db* mice exhibited an altered gut microbial composition, increased intestinal permeability, and higher plasma LPS levels. In addition, *db/db* mice presented increased infarct volumes and higher expression levels of LPS, TLR4, and inflammatory cytokines in the ischemic brain, as well as more severe neurological impairments and reduced survival rates after MCAO. Oral administration of a non-absorbable antibiotic modulated the gut microbiota and improved metabolic endotoxemia and stroke outcomes in *db/db* mice; these effects were associated with reduction of LPS levels and neuroinflammation in the ischemic brain. These data suggest that targeting metabolic endotoxemia may be a novel potential therapeutic strategy to improve stroke outcomes.

Keywords: Gram-negative bacteria, lipopolysaccharide, metabolic endotoxemia, stroke, type 2 diabetes.

Introduction

Lipopolysaccharide (LPS), often referred to as endotoxin, is a major component of the outer membrane of Gram-negative bacteria. Lipopolysaccharide is a potent inflammatory stimulus for the innate immune response via toll-like receptor (TLR) 4 activation.[1] Inflammation plays important roles in the development of strokes and is also implicated in the pathophysiology of ischemic lesions, as well as in the overall outcome after stroke.[2] According to the Bruneck Study, an increased plasma LPS level constitutes a substantial risk factor for incident carotid atherosclerosis and cardiovascular disease.[3] Furthermore, a higher plasma LPS level is associated with worse short-term outcomes in patients with acute ischemic stroke.[4] Experimental studies have demonstrated that systemic LPS administration exacerbates brain damage after cerebral ischemia.[5,6]

The human intestine is home to a vast number of bacteria, and the intestinal barrier prevents under physiological conditions, the passage of harmful luminal contents such as LPS.[7] Recently, growing evidence has emerged that chronic exposure of the host to gut microbiota-derived LPS links to metabolic disorders, a condition referred to as metabolic endotoxemia.[8] Alteration of gut microbiota (gut dysbiosis) and impairment of intestinal barrier functions lead to translocation of LPS into the circulatory system and

contribute to the pathogenesis of type 2 diabetes via the activation of proinflammatory cascades in adipose tissues.[8] Furthermore, increased intestinal permeability and increased circulating LPS levels have been reported to contribute to the pathogenesis of nonalcoholic steatohepatitis by inflammatory liver damage.[9] In patients with type 2 diabetes, increased serum levels of LPS and proinflammatory cytokines have been reported.[10] In addition, we have previously demonstrated increased inflammatory marker levels concurrent with gut dysbiosis and higher LPS-binding protein concentrations, which reflect circulating LPS levels.[11] These findings indicate the importance of gut microbiota-derived LPS as a trigger for inflammatory responses in the host in type 2 diabetes.

Stroke commonly occurs in patients with cardiovascular risk factors. Type 2 diabetes is observed in approximately 60% of patients with acute ischemic stroke.[12] Type 2 diabetes is not only associated with a significantly increased stroke risk but also an early progression of ischemic lesions[13] and worse functional outcomes.[14] However, establishment of clinically effective neuroprotective therapies has been challenging.[15,16]

Hence, to study whether metabolic endotoxemia could be a therapeutic target to improve stroke outcome, we investigated the effects of metabolic endotoxemia on acute ischemic brain injury after experimental

stroke in a murine model of type 2 diabetes. We hypothesized that metabolic endotoxemia will promote LPS-induced neuroinflammation and affect the outcome after stroke.

Materials and methods

Experimental animals

All animal experiments were approved by the Juntendo University Animal Ethics Committee (No. 1176) and were in accordance with Animal Research: Reporting in Vivo Experiments (ARRIVE) reporting guidelines for the care and use of laboratory animals. We strictly followed *the National Institutes of Health Guide for the Care and Use of Laboratory Animals*.

Leptin receptor-deficient (*db/db*) mice exhibit features of type 2 diabetes.[9] We purchased 8-week-old male *db/db* mice (n = 63) and lean, phenotypically normal littermates (*db/+* mice) (n = 65) from Charles River Laboratories Japan, Inc. Mice were maintained on a 12-h light/dark cycle with *ad libitum* access to standard chow and tap water. In some animals, we used polymyxin B, a non-absorbable antibiotic, which selectively acts on Gram-negative bacteria. In the polymyxin B-treatment group, mice received 1 mg of polymyxin B (WAKO, Osaka, Japan) dissolved in 0.2 mL of distilled water once daily by oral gavage for one week. In

the non-treatment group, mice received 0.2 mL of distilled water once daily by oral gavage for one week. The treatment schedule was identical for both groups. This treatment began when mice were 11 weeks old (Figure 1(a)).

Polymyxin B plasma concentration

Plasma samples of *db/db* mice were collected 4 h after oral administration of polymyxin B. Polymyxin B standard (Hycult Biotech, PA, USA) and samples were analyzed using an enzyme-linked immunosorbent assay (ELISA). Briefly, plasma samples were added to LPS-coated plates (Hycult Biotech) and incubated with 200 μL of blocking buffer for 1 h. Subsequently, anti-polymyxin B immunoglobulin M (IgM; Hycult Biotech) was added and incubated for 1 h. Anti-mouse IgM horseradish peroxidase (Hycult Biotech) was used as a secondary antibody. Finally, 3,3',5,5'-tetramethylbenzidine (TMB) (Scy Tech, West Logan, UT, USA) and a stop solution were added to each well. Optical density values at 450 nm minus those obtained at 570 nm were analyzed.

Middle cerebral artery occlusion (MCAO)

Mice were anesthetized with 4.0% isoflurane (Abbott Japan Co., Ltd., Tokyo, Japan) and maintained with 1.0%–1.5% isoflurane in 70% N_2O and 30% O_2 using a small-animal anesthesia system. All surgical instruments were sterilized prior to surgery. Before any incision was made, the area was swabbed with ethanol. Transient cerebral focal ischemia was induced by MCAO for 60 min using an intraluminal filament technique as described previously (Figure 1(a)).[17] Briefly, the left common carotid artery and the left external carotid artery were exposed and ligated after a ventral midline neck incision. A silicon-coated nylon monofilament was inserted through the left common carotid artery into the left internal carotid artery to occlude the left MCA. After 60 min of occlusion, the monofilament was withdrawn for reperfusion. Regional cerebral blood flow (rCBF) was measured in the left temporal window on laser Doppler-flowmetry (FLOW-C1; Omegawave Inc., Tokyo, Japan) before, during, and 24 h after MCAO. We excluded mice (n = 5) in which the reduction in rCBF of the laser Doppler signal was below 60%, when compared with the preischemic state. During the procedure, a core body temperature of 37.0 ± 0.5 °C was maintained using a heating pad.

Functional outcome testing and 7-day survival rate

Neurological severity was assessed 1 h and 24 h after MCAO on a scale of 0 (normal) to 18 (maximal deficit) using the Modified Neurological Severity Score, which is a composite of motor (muscle status, abnormal movement, and balance), sensory (visual, tactile, and proprioceptive), and reflex test scores.[18] In the severity scores of injury, 1 score point is awarded for the inability to perform the test or for the lack of a tested reflex; thus, the higher the score, the more severe the injury. The 7-day survival rate for each group was determined using the Kaplan-Meier analysis.

LPS administration

In a subgroup of polymyxin B-treated *db/db* mice, LPS (*Escherichia coli* 0111: B4, 100 μg/kg; Sigma-Aldrich Co., St. Louis, MO, USA) dissolved in sterile saline or vehicle (sterile saline) was injected intraperitoneally 30 min before the induction of MCAO as previously described.[5,6]

Biochemical assays

Blood samples were collected from 12-week-old *db/+* and *db/db* mice treated with either distilled water or

polymyxin B (Figure 1(a)). Plasma glucose levels before MCAO were measured using a blood glucose meter (Johnson & Johnson, New Brunswick, NJ, USA). Plasma cytokine levels before MCAO were measured using ELISA. These measured cytokines included tumor necrosis factor-α (TNF-α) (LifeSpan BioSciences, Seattle, USA; sensitivity 15.63 pg/mL), interleukin (IL)-1β (R&D Systems, Minneapolis, MN, USA; sensitivity 2.31 pg/mL), and IL-6 (R&D Systems; sensitivity 1.6 pg/mL). Plasma LPS levels were measured before and 24 h after MCAO. Plasma samples for LPS measurements were stored in LPS-free glass tubes and heated to 70 °C for 5 min before LPS measurement. Plasma LPS concentrations were determined using a kit based on a Limulus amebocyte extract (LPS kit, Cusabio, USA).

Intestinal permeability

Intestinal permeability was measured as described previously.[8,19] Briefly, mice that had fasted for 6 h received 4,000 kDa fluorescein isothiocyanate (FITC)-dextran (440 mg/kg body weight, 100 mg/mL) dissolved in deionized water by oral gavage before or 3 h after MCAO. The mice were anesthetized 1 h after oral gavage, and a cardiac puncture was performed to collect blood. Plasma samples were diluted in equal volumes of phosphate-buffered saline (PBS; pH 7.4) and analyzed for FITC-dextran content with a

fluorescence spectrophotometer (Mithras^2 LB 943 microplate reader, Berthold Technologies, Bad Wildbad, Germany) at an excitation wavelength of 485 nm and an emission wavelength of 528 nm.

16S and 23S rRNA-targeted quantitative reverse transcription (qRT)-polymerase chain reaction (PCR)

Fecal samples were collected from 12-week-old *db/+* and *db/db* mice treated with either distilled water or polymyxin B, before and 24h after MCAO (Figure 1(a)). The composition of fecal gut microbiota was determined via 16S and 23S rRNA-targeted qRT-PCR using the Yakult Intestinal Flora-SCAN analysis system (YIF-SCAN®, Yakult Honsha Co., Ltd., Tokyo, Japan) as previously described.[20] The sequences of primers used for these analyses are listed in Supplementary Table 1.

Tissue processing

Mice were anesthetized by an intraperitoneal injection of pentobarbital (50 mg/kg) 24 h after MCAO and transcardially perfused with 20 mL ice-cold PBS to remove blood from the brain capillaries as described previously.[21] The brains turned completely white. For histological analysis, brains were subsequently perfused with 4% paraformaldehyde in PBS, which was then removed, and brains were post-fixed in the

same fixative overnight at 4 °C. Subsequently, each brain was soaked overnight in 30% sucrose in PBS. For western blot analysis and ELISA, brains were removed immediately after PBS perfusion and stored at −80 °C.

Measurement of infarct volume

For infarct quantification, forebrains were coronally sectioned into 20-µm-thick sections on a cryostat (Model CM 1900, Leica, Germany) separated by 1-mm intervals. Sections were stained with Cresyl Violet and scanned using the AxioVision software (Carl Zeiss, Jena, Germany). Image analyses were performed using the ImageJ software (National Institutes of Health; https://imagej.nih.gov/ij/). Infarct volumes and hemispheric volumes were calculated using numerical integrations of the respective areas for all sections and the distance between them. Corrected infarct volumes were calculated to compensate for the effect of brain edema using the following equation: corrected infarct volume = infarct volume – (ipsilateral hemisphere volume – contralateral hemisphere volume).[22]

Blood-brain barrier evaluation

To evaluate the permeability of the blood-brain barrier, brain sections (20-μm-thick) collected 24 h after MCAO were incubated in 3% H_2O_2 followed by blocking with 10% bovine serum albumin (Sigma-Aldrich) in PBS. Afterward, sections were incubated overnight at 4 °C with donkey anti-mouse IgG (1:300 dilution; Vector Laboratories, Burlingame, CA, USA). Immunoreactivity was visualized using the avidin-biotin complex method (Vectastain ABC kit, 1:400 dilution; Vector Laboratories). IgG was quantified for blood-brain barrier disruption using Image J.

Immunohistochemical analysis

Immunohistochemical analysis was performed on brains harvested 24 h after MCAO. Sections of forebrains (20-μm-thick) were incubated with anti-ionized calcium-binding adapter molecule antibody (Iba1, 1:500 dilution; WAKO), treated with biotinylated secondary antibody (1:300 dilution; Vector Laboratories), and subsequently processed with an avidin-biotinylated peroxidase complex (Vectastain ABC kit; 1:400 dilution; Vector Laboratories). To assess microglia/macrophage activation, the total number of Iba1-stained cells as well as the Iba1-stained area were calculated at the ischemic boundary area (0.25 mm^2) 24 h after

MCAO using ImageJ as previously described.[23]

Double immunofluorescence staining was performed by simultaneous incubation of the sections with the following primary antibodies overnight at 4 °C: anti-*Escherichia coli* LPS (1:100 dilution; Abcam) and anti-*E. coli* K99 (1:100 dilution; Lifespan, Providence, RI, USA), anti-TLR4 (1:100 dilution; Santa Cruz Biotechnology), anti-Iba1 (1:100 dilution; Abcam), anti-NeuN (neuron) (1:100 dilution; Abcam), anti-CD31 (endothelial cells) (1:25 dilution; Abcam), anti-glial fibrillary acidic protein (GFAP) (1:500 dilution; Abcam), and anti-transmembrane protein 119 (TMEM119) (1:150 dilution; Abcam). Thereafter, sections were incubated with a FITC-conjugated secondary antibody (Jackson ImmunoResearch, Baltimore, USA) for the identification of *E. coli* LPS (1:250 dilution), *E. coli* K99 (1:250 dilution), or TLR4 (1:500 dilution), and a Cy™3-conjugated secondary antibody (Jackson ImmunoResearch) for the identification of Iba1 (1:1000 dilution), NeuN (1:500 dilution), CD31 (1:500 dilution), GFAP (1:500 dilution) or TMEM119 (1:1000 dilution). Sections were covered with Vectashield mounting medium (Vector Laboratories), and immunofluorescent images were obtained using a laser-scanning microscope (model LSM780, Carl Zeiss). In immunohistochemical analyses, positively stained cells in the ischemic boundary area (0.25 mm^2) were counted in three sections from each mouse using the ZEN 2011 software (Carl Zeiss). TLR4 expression

was quantified by measuring the percentage of TLR4 immunostaining area in Iba1-, NeuN-, and CD31-positive cells, and the percentage of TMEM119-positive microglia in Iba1-positive cells was quantified using ImageJ. All immunohistochemical data were analyzed in the ipsilateral hemisphere in three coronal sections at +0.4 mm, +0.8 mm, and +1.2 mm from the bregma. Immunopositive cells were counted manually by a researcher who was blinded to the experimental conditions. The average cell number of all the sections was used as the cell number per mouse.

Western blot analysis

Mouse brain samples were obtained 24 h after reperfusion. Samples were homogenized with lysis buffer (CelLytic MT Cell Lysis Reagent; Sigma-Aldrich Co., St. Louis, MO, USA) containing a protease inhibitor cocktail (Complete Mini, EDTA-free; Roche). Homogenized samples were centrifuged at 12000 × *g* for 20 min, and pellets were discarded. Aliquots of supernatants containing 25 μg of protein were subjected to 4%–15% sodium dodecyl sulfate-polyacrylamide gel electrophoresis (SDS-PAGE) and transferred to polyvinylidene difluoride membranes (Bio-Rad Laboratories, Hercules, CA, USA). The membranes were blocked in Brockace (Dainichi-Seiyaku, Gifu, Japan) for 60 min at room temperature. Subsequently,

membranes were incubated overnight at 4 °C with antibodies against TLR4 (1:500 dilution; Santa Cruz Biotechnology, Santa Cruz, CA, USA), LPS (1:500 dilution; Abcam, Cambridge, MA, USA), and β-actin (1:5000 dilution, Abcam) followed by incubation with secondary antibodies and visualization via enhanced chemiluminescence (GE Healthcare UK, Little Chalfont, Buckinghamshire, UK).

Brain inflammatory cytokine measurement

Mouse brain samples were obtained 24 h after reperfusion. Samples were homogenized with PBS and centrifuged at 5000 × *g* for 5 min. The supernatant was collected and assayed immediately. Levels of inflammatory cytokines including TNF-α (LifeSpan BioSciences; sensitivity 15.63 pg/mL), IL-1β (R&D Systems; sensitivity 2.31 pg/mL), and IL-6 (R&D Systems; sensitivity 1.6 pg/mL) were measured using ELISA according to the manufacture's protocol.

Statistical analysis

Power estimates were calculated with the values $\alpha = 0.05$ and $\beta = 0.8$ to obtain group sizes appropriate for detecting effect sizes in the range of 30%–50% for in vivo models. Goodness-of-fit to a normal distribution

was assessed by the Shapiro-Wilk test. Data are presented as mean ± standard deviation (SD). One-way analysis of variance with Tukey's HSD *post hoc* tests was used to determine the significant differences between groups. Wilcoxon rank-sum test was used to determine the significant differences in neurological severity scores. Statistical analyses were performed using JMP 12.0.1 software (SAS Inc., Cary, NC, USA). A value of $P < 0.05$ was considered to indicate statistical significance. All experiments and measurements, including behavior outcome assessment, infarct volume measurement, and histological analysis, were performed in a blinded and randomized manner.

Results

Metabolic endotoxemia is associated with a worse stroke outcome

Male 12-week-old *db/db* mice showed higher levels of blood glucose (Figure 1(b)); inflammatory cytokines such as TNF-α, IL-1β, and IL-6 (Figure 1(c)); and body weight (Figure 1(d)) than *db/+* mice before stroke induction. We orally administered polymyxin B and measured its plasma concentrations in *db/db* mice and confirmed that polymyxin B was not absorbed from the intestine (data not shown). *Db/db* mice treated with polymyxin-B had glucose levels (Figure 1(b)) and body weight (Figure 1(d)) similar to those in untreated

db/db mice and higher than those in *db/+* mice. However, the levels of TNF-α, IL-1β, and IL-6 in polymyxin B-treated *db/db* mice were similar to those in *db/+* mice and lower than those in untreated *db/db* mice (Figure 1(c)). Furthermore, *db/db* mice showed higher plasma LPS levels than *db/+* mice or *db/db* mice treated with polymyxin B (Figure 1(e)), accompanied by an increased intestinal permeability (Figure 1(f)) reflecting metabolic endotoxemia. To evaluate changes in gut microbiota composition, we analyzed bacterial 16S and 23S rRNA in feces of *db/db* and *db/+* mice (Figure 1(g), Supplementary Figure. 1(a), and Supplementary Table 2). The fecal counts for *Atopobium* cluster, *Enterobacteriaceae*, and *Enterococcus* were higher, whereas the count for *Clostridium perfringens* was lower in *db/db* mice than in *db/+* mice. *Bifidobacterium* was undetectable in *db/db* mice. Polymyxin B administration attenuated the fecal count of *Enterobacteriaceae* in *db/db* mice. Although, the number of some bacteria differ among *db/+*, *db/db*, and polymyxin-B treated *db/db* mice, the total bacterial count was not different among these mice. This is due to the fact that the bacterial number of predominant bacteria including the *Clostridium coccoides* group, *Clostridium leptum* subgroup, *Bacteroides fragilis* group, and *Lactobacillus* that corresponds to approximately 80% to 90% of all bacteria, was not different among the groups (Supplementary Figure 2). Subsequently, we induced transient MCAO in *db/+*, *db/db*, and polymyxin B-treated *db/db* mice.

Physiological parameters such as weight loss (Supplementary Figure 3(a)) and rCBF (Supplementary Figure 3(b)) did not differ among the groups. Plasma LPS levels (Supplementary Table 3) and intestinal permeability (Supplementary Table 4) after MCAO were higher than those before MCAO in all groups. In addition, *db/db* mice showed higher plasma LPS levels (Figure 2(a)) and intestinal permeability (Figure 2(b)) after MCAO among the groups. Differences were observed in bacterial number and detection rates in some bacteria between those before and after MCAO (Supplementary Figure 4). Particularly, the bacterial number of *Lactobacillus* was higher after MCAO than before MCAO in all groups. Furthermore, the bacterial number and detection rates of *Bifidobacterium* in *db/+* and polymyxin B-treated *db/db* mice, *Enterococcus* in *db/db* mice, and *Atopobium* cluster, *Clostridium perfringens*, and *Enterobacteriaceae* in all groups, were lower after MCAO compared to those before MCAO. However, the gut microbiota compositions after MCAO were not different among *db/+*, *db/db*, and polymyxin B-treated *db/db* mice (Figure 2(c), Supplementary Table 5 and Supplementary Figure 1(b)).

Infarct volumes (Figure 3(a)) and blood-brain barrier damage (Figure 3(b)) were greater in *db/db* mice than in *db/+* mice 24 h after MCAO. In addition, Iba1-positive microglia/macrophages in peri-infarct areas in *db/+* mice were highly ramified, whereas those in *db/db* mice exhibited a less ramified and even amoeboid

cell morphology (Figure 3(c)). The number of Iba1-positive cells and Iba1-immunoreactive areas were higher in *db/db* than in *db/+* mice in peri-infarct areas 24 h after MCAO (Figure 3(c)). To analyze Iba1-positive cells in more detail, we performed immunohistochemical analysis using TMEM119, which is a specific marker of the tissue resident microglia (Figure 3(d)). Total number of both TMEM119-positive and TMEM119-negative cells were higher in *db/db* than *db/+* mice in the peri-infarct area 24 h after MCAO (Figure 3(e)). The percentage of TMEM119-positive cells in the Iba1-positive cells was approximately 60% in both groups (Figure 3(e)). Additionally, *db/db* mice showed higher neurological severity scores 24 h after MCAO (Figure 3(f)) and a poorer 7-day survival rate (Figure 3(g)) than *db/+* mice. However, polymyxin B treatment partially reduced the infarct volumes (still increased in comparison to *db/+* mice) (Figure 3(a)) and blood-brain barrier damage (Figure 3(b)), as well as changed the morphology of Iba1-positive cells to a ramified phenotype (Figure 3(c), decreased Iba1-positive cell number and areas (Figure 3(c)), and improved neurological function 24 h after MCAO (Figure 3(f)) and 7-day survival (Figure 3(g)) in *db/db* mice.

Because polymyxin B treatment attenuated the circulating LPS levels and ameliorated the stroke outcome in *db/db* mice, we examined the direct impact of LPS on stroke outcome in *db/db* mice. In polymyxin B-

treated *db/db* mice, intraperitoneal LPS administration before MCAO increased the infarct volume (Figure 3(h)) and number of Iba1-positive cells and Iba1-immunoreactive areas in the peri-infarct area (Figure 3(i)), as well as the neurological severity score (Figure3(j)), 24 h after MCAO.

In the normoglycemic control *db/+* mice, infarct volume (Figure 3(a)) and stroke outcomes such as neurological severity score (Figure 3(f)) and survival rate after MCAO (Figure 3(g)) were comparable to those in C57BL/6 mice, which has been reported in our previous study.[17] Oral gavage of polymyxin B did not show any effects on plasma LPS levels (Supplementary Figure 5(a)), intestinal permeability (Supplementary Figure 5(b), infarct volumes 24 h after MCAO (Supplementary Figure 5(c)) and neurological functions 1 h and 24 h after MCAO (Supplementary Figure 5(d)) in *db/+* mice. Additionally, the bacterial counts did not change between *db/+* and polymyxin B-treated *db/+* mice 24 h after MCAO (Supplementary Figure 5(e)).

LPS and neuroinflammation in the ischemic brain

Since we found that metabolic endotoxemia was associated with worse stroke outcome, we analyzed the presence of LPS in the brain 24 h after ischemia. Western blot analysis revealed that LPS levels were higher

in the ischemic hemispheres of *db/db* mice compared to those of *db/+* mice; LPS levels were attenuated by polymyxin B treatment in *db/db* mice (Figure 4(a)). In all groups, LPS was not detected in the contralateral, non-ischemic hemispheres (Supplementary Figure 6(a)). Next, we examined the expression levels of TLR4, an LPS receptor, and inflammatory cytokines in the ischemic brain. Expression levels of TLR4 (Figure 4(b)), TNF-α, IL-1β, and IL-6 (Figure 4(c)) were higher in *db/db* mice than in *db/+* mice, but lower in polymyxin B-treated *db/db* mice than in untreated *db/db* mice. The expression levels of TLR4 and these inflammatory cytokines in the contralateral hemispheres did not change among these groups (Supplementary Figure 6(b) and (c)).

Localization of LPS, E. coli K99 pili protein, and TLR4 in the ischemic brain

We examined the localization of LPS and *E. coli* (which belongs to the *Enterobacteriaceae* family) K99 pili protein in the brain 24 h after ischemia. The immunohistochemical analysis demonstrated that LPS (Figure 5(a)) and *E. coli* K99 pili protein (Figure 5(b)) were localized in the peri-infarct area in Iba1-positive microglia/macrophages, neurons, and endothelial cells, but not in astrocytes. High magnification images showed that LPS (Figure 5(a)) and *E. coli* K99 pili protein (Figure 5(b)) were adherent on the surface of

Iba1-positive microglia/macrophages, neurons, and endothelial cells. Neither LPS nor *E. coli* K99 pili protein was detected in the contralateral hemispheres (data not shown). We also observed in the peri-infarct area, TLR4 immunoreactivity in Iba1-positive microglia/macrophages, neurons, and endothelial cells, but not in astrocytes (Figure 5(c)). The percentages of TLR4-immunoreactive areas in these cells were higher in *db/db* mice compared to *db/+* mice and polymyxin B-treated *db/db* mice (Figure 5(d)).

Discussion

The present study demonstrates that metabolic endotoxemia is negatively associated with stroke outcome. Increased intestinal permeability and circulating LPS levels were associated with increased levels of LPS, TLR4, and inflammatory cytokines in the ischemic brain in diabetic mice (Figure 6). Moreover, gut microbiota modulation with a non-absorbable antibiotic polymyxin B attenuated LPS levels in the circulation, thereby in the ischemic brain and improved the stroke outcome. Notably, LPS administration attenuated the positive effects of gut microbiota modulation with the antibiotic on stroke outcomes. Additionally, polymyxin B treatment had no effect on stroke outcomes in control mice, in which, circulating LPS levels were much lower than in diabetic mice. These findings suggest an association between

metabolic endotoxemia and the pathophysiology of acute ischemic brain injury via the Gram-negative bacterial toxin LPS in diabetic mice.

In the present study, *db/db* mice showed enrichment of fecal *Enterobacteriaceae*. *Enterobacteriaceae* are a large family of Gram-negative bacteria that includes opportunistic pathogens such as *E. coli*, *Klebsiella*, and *Salmonella*. Consistent with the results of our study, a previous study in *db/db* mice also showed an increase in *Proteobacteria* (this phylum contains *Enterobacteriaceae*).[24] An increase in the number of *Proteobacteria* is observed during gut dysbiosis in several diseases including inflammatory bowel disease, colorectal cancer, metabolic syndrome, and type 2 diabetes.[25] In addition, a previous clinical study showed that acute stroke patients had a more abundant presence of *Enterobacter* (which belongs to the *Enterobacteriaceae* family).[26] However, dysbiosis with expansion of the *Burkholderiaceae* family, which belongs to the *Proteobacteria*, is associated with neuroprotective effects on ischemic cerebral injury in mice.[27]

Polymyxin B is one of the primary classes of antibiotics with activity against most Gram-negative bacteria.[28] In our bacterial analysis, Gram-negative bacteria included the *Bacteroides fragilis* group, *Prevotella*, *Enterobacteriaceae*, and *Pseudomonas*. However, *Prevotella* and *Pseudomonas* were

undetectable in all groups. Polymyxin B attenuated *Enterobacteriaceae*. However, polymyxin B had no effects on the bacterial counts of *Bacteroides fragilis*, known to be resistant to this antibiotic.[29] We showed that increased fecal levels of *Enterobacteriaceae* were associated with increases in circulating LPS levels concurrent with increased intestinal permeability before stroke induction. Emerging evidence has revealed that gut microbiota has potent effects on intestinal permeability. The proliferation of *Enterobacteriaceae* leads to an increase in luminal LPS content in the gut, which results in changes in tight junction proteins and an increase in intestinal permeability through TLR4-induced inflammation.[30] The substantial changes in expression/distribution of tight junction proteins with enhanced intestinal permeability have been shown to lead to an abnormal leakage of bacterial LPS into the circulatory system in *db/db* mice.[9] We also found that higher plasma LPS levels were associated with increasing inflammatory cytokine levels, while gut microbiota modulation reduced circulating LPS levels and inflammatory signaling. These findings are consistent with a previous report investigating endotoxemia and systemic inflammation using *db/db* mice.[9] Furthermore, our study found that *Bifidobacterium* was undetectable in feces of *db/db* mice before stroke induction. Decreased *Bifidobacterium* levels have been implicated in intestinal barrier dysfunction and LPS translocation.[31,32] Therefore, the reduction in *Bifidobacterium* may also have increased the levels of

circulating LPS in *db/db* mice in our study. Additionally, our study showed that the number of *Clostridium perfringens* in *db/db* mice was lower than that in *db/+* mice. This finding is in line with a previous study, which showed a lower amount of *Clostridium perfringens* in obese subjects compared to normal-weight people.[33] Thus, a decrease in the number of *Clostridium perfringens* may be associated with an obese phenotype. However, these Gram-positive bacteria were not affected by polymyxin B treatment in *db/db* mice, suggesting *Clostridium perfringens* may not have contributed to endotoxemia before stroke induction in these mice.

Lately, special focus has been placed on the gut-brain axis in ischemic stroke pathophysiology. Gut microbiota have been implicated in ischemic brain injury after stroke via the regulation of intestinal T cells.[27,34] Additionally, stroke causes specific changes in gut microbiota, which in turn contributes to stroke outcomes.[34,35,36] Stroke also promotes the translocation and dissemination of bacteria from host gut microbiota as a mechanism leading to post-stroke infection.[19] Recently, Gram-negative bacteria-derived LPS has been implicated in the neuropathology of the human brain. For example, LPS and the K99 pili protein of Gram-negative *E. coli* bacteria were detected at higher levels in brains of patients with Alzheimer's disease compared to controls and were colocalized with amyloid β in amyloid plaques and

around vessels.[37] However, the origin of these bacterial molecules in the brain is currently not well understood.

In the current study, we determined the presence of LPS and *E. coli* K99 pili protein in the ischemic brain 24 h after cerebral ischemia. Lipopolysaccharide levels in the ischemic brain were attenuated by oral gavage of the non-absorbable antibiotic, polymyxin B in *db/db* mice. These findings were associated with suppression of fecal *Enterobacteriaceae* counts, intestinal permeability, and circulating LPS levels before stroke induction. We also found that intestinal permeability was further enhanced after MCAO in all group mice. These findings were in line with a previous study investigating the intestinal permeability in mice subjected to MCAO.[19] Importantly, our study showed that *db/db* mice had the most prominent increase of plasma LPS levels and intestinal permeability after MCAO among groups. Our study also showed that stroke induced certain changes in gut microbiota, particularly an increase in *Lactobacillus,* which is in line with a previous study.[36] Additionally, some non-predominant bacteria were reduced or undetectable after MCAO. Reduction in species diversity is a key feature of dysbiosis after stroke.[34] However, the gut microbiota compositions after MCAO were not different among *db/+*, *db/db*, and polymyxin B-treated *db/db* mice. Therefore, our findings suggest that stroke has a greater impact on gut microbiota composition

than the phenotypes such as type 2 diabetes.

Toll-like receptor 4 plays an important role in post-stroke inflammation and contributes to the progression of brain damage, whereas genetic deletion of TLR4 significantly reduces the infarct volume.[38] Damage-associated molecular patterns released from injured neurons such as high mobility group box 1[39] and peroxiredoxin family proteins[40] activate TLR4 in the brain after cerebral ischemia. Among the members of the TLR family, TLR4 is mainly involved in LPS-mediated inflammatory responses.[1] In the present study, TLR4 and inflammatory cytokine levels in the ischemic brain were significantly higher in *db/db* compared to *db/+* mice. These findings were associated with LPS levels in ischemic brains; the reduction in LPS levels in polymyxin B-treated *db/db* mice decreased TLR4 and inflammatory cytokine levels. We also found that *db/db* mice showed higher levels of plasma inflammatory cytokines compared with *db/+* and polymyxin B-treated *db/db* mice. Therefore, although ischemic injury increases TLR4 activation,[39,40] it is also possible that influx of LPS, as well as extravasation of plasma inflammatory cytokines into the ischemic brain, also contribute to neuroinflammation.

In the peri-infarct area, we found that LPS and *E. coli* K99 pili protein were adherent on the surface of Iba1-positive microglia/macrophages, endothelial cells, and neurons, but not in astrocytes. Furthermore,

Iba1-positive microglia/macrophages, endothelial cells, and neurons, except astrocytes expressed TLR4. Immunoreactive areas of TLR4 in these cells were higher in *db/db* mice compared to *db/+* and polymyxin B-treated *db/db* mice, suggesting TLR4 activation was pronounced in *db/db* mice. Among the major non-neuronal cell types in the brain, microglia expressed high levels of TLR4, whereas astrocytes expressed none.[41] Furthermore, microglia are the only glial cells that bind LPS.[41] These findings suggest that microglia/macrophages contribute to LPS-induced neuroinflammation. The question of TLR4 expression in astrocytes has not been undeniably clarified, since in different studies TLR4 was either absent[41,42] or present.[43] These inconsistencies in the reported expression patterns may be related to differences in the experimental paradigms and immunoprobes used. Endothelial cells also express TLR4[44] and produce cytokines in response to LPS stimulation.[45] Additionally, LPS has been reported to induce inflammatory cytokine production in neurons via TLR4 activation.[46]

Our study showed that Iba1-positive cells in *db/+* mice were characterized by a highly ramified shape, whereas those in *db/db* mice showed a less ramified or amoeboid cell morphology, reflecting their activation status.[47] The origin of cells identified by Iba1 could either be activated brain-resident microglia or macrophages derived from circulating monocytes.[47] The TMEM119 is a recently identified highly

specific cell-surface marker of microglia that is not expressed by macrophages or other immune or neural cell types.[48] Our study showed that approximately 60% of Iba1-positive cells expressed TMEM119 in both *db/+* and *db/db* mice. This is in line with a pathological study of human brains showing that 43% of Iba1-positive cells at the edge of acute ischemic lesions expressed TMEM119.[49] Altogether, these findings suggest that Iba1-positive cells consist in part of resident microglia, and in part of infiltrating macrophages in per-infarct areas of acute cerebral ischemia.

Although systemic LPS administration has been shown to disrupt the blood-brain barrier,[50] we did not see significant differences in IgG staining in the contralateral, non-ischemic hemispheres among *db/+*, *db/db,* and polymyxin B-treated *db/db* mice. Indeed, LPS was not detected and levels of TLR4 and inflammatory cytokines were not different in the non-ischemic hemispheres in all these mice. This might be explained by differences in experimental models (systemic LPS administration vs. metabolic endotoxemia), which may result in different effects on the blood-brain barrier.

Interestingly, LPS preconditioning provides neuroprotective effects via several mechanisms including proinflammatory cytokine production. Induction of TNF-α by LPS administration before stroke causes ischemic tolerance by suppressing the TNF-α response to cerebral ischemic injury.[51] Furthermore, LPS pre-

treatment reduces *N*-methyl-D-aspartate-mediated cerebral injury by inducing nitric oxide and cGMP.[52] Thus, LPS can be neuroprotective when it is administered under optimal conditions (dose and timing). However, our study indicated that chronic exposure to LPS may be deleterious by increasing neuroinflammation after stroke.

Among the cardiovascular risk factors, type 2 diabetes is considerably associated with poor functional outcomes after stroke.[14] Yet, controlling post-stroke hyperglycemia has no effect on the outcome in experimental animal models[15] or stroke patients.[16] In the present study, we demonstrated that the reduction in circulating LPS levels was associated with an attenuation of inflammatory cytokine production, as well as with improvements in neurological functions and survival after stroke, without influencing plasma glucose levels in a mouse model of type 2 diabetes. Although our study demonstrated that polymyxin B was effective to reduce the bacterial counts of *Enterobacteriaceae* and thereby decrease circulating LPS levels, antibiotic treatment may not be suitable for the clinical setting due to potential undesirable side effects associated with antibiotic treatment and the risk of emergence of antibiotic-resistant bacteria. Experimental studies have shown that supplementation of *Bifidobacterium*[31] or oligofructose[32] decreases plasma LPS levels. Thus, the administration of pro- or prebiotics may be a potential treatment option to

improve stroke outcomes by preventing LPS translocation in patients with type 2 diabetes.

Although interspecies differences should always be considered, the murine gut has successfully been used as a model to investigate the role of gut microbiota in complex human disorders, including post-stroke infections, obesity, and diabetes.[8,19]

The present study had some limitations. First, although we used sterile techniques, LPS could have contaminated tissue samples. However, LPS levels were consistently higher in *db/db* compared to *db/+* and polymyxin B-treated *db/db* mice, despite using the same techniques in all groups. In addition, LPS was not detected in non-ischemic hemispheres. Second, the effects of other bacteria, not included in our microbiota analysis, need to be further investigated. However, the rRNA-targeted qRT-PCR used in this study enables high-resolution quantification of targeted bacterial populations including potentially pathogenic bacteria which might not be quantified efficiently, by either routine DNA-based PCR or next-generation sequencing methods due to their low sensitivity.[53,54] Third, we focused on LPS in the present study, but further studies are needed to examine the potential importance of other bacteria-derived molecules such as peptidoglycan in stroke pathophysiology. Additionally, as gut microbiota contributes to ischemic cerebral injury by regulating peripheral immune cells,[27,34] analyzing the impact of gut dysbiosis and polymyxin B treatment

on peripheral immune cells is crucial. Fourth, since parameters were measured post-stroke and correlated with the size of the lesion, they did not address the direct role of endotoxemia. Experiments with TLR4 knock-out mice would provide more details about the interactions between endotoxemia and neuroinflammation. Additionally, our study showed that *db/db* mice had greater ischemic damage compared to *db/+* mice 24 h after MCAO. To elucidate how the infarct develops over time, further investigations are needed at earlier time points. Finally, our results are limited to young male mice and may not be applicable to old or female mice. In addition, the 12-week-old *db/db* mice used in the current study had extremely high glucose levels, which could be responsible for the poor survival rate after stroke, and this limited the ability to conduct long-term studies on the effect of polymyxin B or the effects of polymyxin B administration after stroke. Particularly, it would be of interest to examine whether LPS that remains in the brain, contributes to poststroke cognitive decline in a similar manner to Alzheimer's disease.[37] In this regard, a milder diabetic model such as high-fat diet fed-mice would be useful in future research.

In conclusion, our study suggests that metabolic endotoxemia is associated with neuroinflammation after transient focal cerebral ischemia in type 2 diabetes. Targeting metabolic endotoxemia might be a novel potential therapeutic strategy to improve stroke outcomes.

Funding

This project was funded by the JSPS KAKENHI grant no. JP15K07439.

Authors' contributions

NK, KY, TK, RT, TU, YY, NH: Conception and experimental design; NK, KY, TK, YU, NM, MT, HS, TI, KN, SM, TT, HT, TA: Experimental work; NK, KY: Interpretation of data and writing of manuscript. All authors discussed the results and provided input regarding the manuscript. All the authors have approved the final version of the manuscript.

Declaration of conflicting interests

The Authors declare that there are no conflict of interest.

Supplementary material

Supplementary material for this paper can be found at the journal website:

http://journals.sagepub.com/home/jcb

References

1. Kawai T and Akira S. The role of pattern-recognition receptors in innate immunity: update on Toll-like receptors. *Nat Immunol* 2010; 11: 373–384.

2. Macrez R, Ali C, Toutirais O, et al. Stroke and the immune system: from pathophysiology to new therapeutic strategies. *Lancet Neurol* 2011; 10: 471–480.

3. Wiedermann CJ, Kiechl S, Dunzendorfer S, et al. Association of endotoxemia with carotid atherosclerosis and cardiovascular disease: prospective results from the Bruneck Study. *J Am Coll Cardiol* 1999; 34: 1975–1981.

4. Klimiec E, Pera J, Chrzanowska-Wasko J, et al. Plasma endotoxin activity rises during ischemic stroke and is associated with worse short-term outcome. *J Neuroimmunol* 2016; 297: 76–80.

5. McColl BW, Rothwell NJ and Allan SM. Systemic inflammatory stimulus potentiates the acute phase and CXC chemokine responses to experimental stroke and exacerbates brain damage via interleukin-1- and neutrophil-dependent mechanisms. *J Neurosci* 2007; 27: 4403–4412.

6. Doll DN, Hu H, Sun J, et al. Mitochondrial crisis in cerebrovascular endothelial cells opens the blood-brain barrier. *Stroke* 2015; 46: 1681–1689.

7. Odenwald MA and Turner JR. The intestinal epithelial barrier: a therapeutic target? *Nat Rev Gastroenterol Hepatol* 2017; 14: 9–21.

8. Cani PD, Bibiloni R, Knauf C, et al. Changes in gut microbiota control metabolic endotoxemia-induced inflammation in high-fat diet-induced obesity and diabetes in mice. *Diabetes* 2008; 57: 1470-1481.

9. Brun P, Castagliuolo I, Di Leo V, et al. Increased intestinal permeability in obese mice: new evidence in the pathogenesis of nonalcoholic steatohepatitis. *Am J Physiol Gastrointest Liver Physiol* 2007; 292: G518–G525.

10. Creely SJ, McTernan PG, Kusminski CM, et al. Lipopolysaccharide activates an innate immune system response in human adipose tissue in obesity and type 2 diabetes. *Am J Physiol Endocrinol Metab* 2007; 292: E740–E747.

11. Sato J, Kanazawa A, Ikeda F, et al. Gut dysbiosis and detection of "live gut bacteria" in blood of Japanese patients with type 2 diabetes. *Diabetes Care* 2014; 37: 2343–2350.

12. Urabe T, Watada H, Okuma Y, et al. Prevalence of abnormal glucose metabolism and insulin resistance among subtypes of ischemic stroke in Japanese patients. *Stroke* 2009; 40: 1289–1295.

13. Tureyen K, Bowen K, Liang J, et al. Exacerbated brain damage, edema and inflammation in type-2 diabetic mice subjected to focal ischemia. *J Neurochem* 2011; 116: 499–507.

14. Tanaka R, Ueno Y, Miyamoto N, et al. Impact of diabetes and prediabetes on the short-term prognosis in patients with acute ischemic stroke. *J Neurol Sci* 2013; 332: 45–50.

15. MacDougall NJ and Muir KW. Hyperglycaemia and infarct size in animal models of middle cerebral artery occlusion: systematic review and meta-analysis. *J Cereb Blood Flow Metab* 2011; 31: 807–818.

16. Johnston KC, Bruno A, Pauls Q, et al. Intensive vs Standard Treatment of Hyperglycemia and Functional Outcome in Patients With Acute Ischemic Stroke: The SHINE Randomized Clinical Trial. *JAMA* 2019; 322: 326-335.

17. Kuroki T, Tanaka R, Shimada Y, et al. Exendin-4 inhibits matrix metalloproteinase-9 activation and reduces infarct growth after focal cerebral ischemia in hyperglycemic mice. *Stroke* 2016; 47: 1328–1335.

18. Chen J, Li Y, Wang L, et al. Therapeutic benefit of intravenous administration of bone marrow stromal cells after cerebral ischemia in rats. *Stroke* 2001; 32: 1005–1011.

19. Stanley D, Mason LJ, Mackin KE, et al. Translocation and dissemination of commensal bacteria in post-stroke infection. *Nat Med* 2016; 22: 1277-1284.

20. Yamashiro K, Tanaka R, Urabe T, et al. Gut dysbiosis is associated with metabolism and systemic inflammation in patients with ischemic stroke. *PLoS One* 2017; 12: e0171521.

21. Gregersen R, Lambertsen K, Finsen B. Microglia and macrophages are the major source of tumor necrosis factor in permanent middle cerebral artery occlusion in mice. *J Cereb Blood Flow Metab* 2000; 20: 53-65.

22. Bastide M, Bordet R, Pu Q, et al. Relationship between inward rectifier potassium current impairment and brain injury after cerebral ischemia/reperfusion. *J Cereb Blood Flow Metab* 1999; 19: 1309-1315.

23. Tanaka M, Ishihara Y, Mizuno S, et al. Progression of vasogenic edema induced by activated microglia under permanent middle cerebral artery occlusion. *Biochem Biophys Res Commun* 2018; 496: 582-587.

24. Geurts L, Lazarevic V, Derrien M, et al. Altered gut microbiota and endocannabinoid system tone in obese and diabetic leptin-resistant mice: impact on apelin regulation in adipose tissue. *Front*

Microbiol 2011; 2: 149.

25. Shin NR, Whon TW and Bae JW. Proteobacteria: microbial signature of dysbiosis in gut microbiota. *Trends Biotechnol* 2015; 33: 496–503.

26. Yin J, Liao SX, He Y, et al. Dysbiosis of gut microbiota with reduced trimethylamine-N-oxide level in patients with large-artery atherosclerotic stroke or transient ischemic attack. *J Am Heart Assoc* 2015; 4: e002699.

27. Benakis C, Brea D, Caballero S, et al. Commensal microbiota affects ischemic stroke outcome by regulating intestinal γδ T cells. *Nat Med* 2016; 22: 516-523.

28. Poirel L, Jayol A and Nordmann P. Polymyxins: antibacterial activity, susceptibility testing, and resistance mechanisms encoded by plasmids or chromosomes. *Clin Microbiol Rev* 2017; 30: 557-596.

29. Kislak JW. The susceptibility of *Bacteroides fragilis* to 24 antibiotics. *J Infect Dis* 1972; 125: 295-299.

30. Kim KA, Gu W, Lee IA, et al. High fat diet-induced gut microbiota exacerbates inflammation and obesity in mice via the TLR4 signaling pathway. *PLoS One* 2012; 7: e47713.

31. Wang Z, Xiao G, Yao Y, et al. The role of bifidobacteria in gut barrier function after thermal injury in rats. *J Trauma* 2006; 61: 650–657.

32. Cani PD, Neyrinck AM, Fava F, et al. Selective increases of bifidobacteria in gut microflora improve high-fat-diet-induced diabetes in mice through a mechanism associated with endotoxaemia. *Diabetologia* 2007; 50: 2374–2383.

33. Zuo HJ, Xie ZM, Zhang WW, et al. Gut bacteria alteration in obese people and its relationship with gene polymorphism. *World J Gastroenterol* 2011; 17: 1076-1081.

34. Singh V, Roth S, Llovera G, et al. Microbiota dysbiosis controls the neuroinflammatory response after stroke. *J Neurosci* 2016;36: 7428–7440.

35. Houlden A, Goldrick M, Brough D, et al. Brain injury induces specific changes in the caecal microbiota of mice via altered autonomic activity and mucoprotein production. *Brain Behav Immun* 2016; 57: 10-20.

36. Stanley D, Moore RJ and Wong CHY. An insight into intestinal mucosal microbiota disruption after stroke. *Sci Rep* 2018; 8: 568.

37. Zhan X, Stamova B, Jin LW, et al. Gram-negative bacterial molecules associate with Alzheimer

disease pathology. *Neurology* 2016; 87: 2324–2332.

38. Caso JR, Pradillo JM, Hurtado O, et al. Toll-like receptor 4 is involved in brain damage and inflammation after experimental stroke. *Circulation* 2007; 115: 1599–1608.

39. Qiu J, Nishimura M, Wang Y, et al. Early release of HMGB-1 from neurons after the onset of brain ischemia. *J Cereb Blood Flow Metab* 2008; 28: 927–938.

40. Shichita T, Hasegawa E, Kimura A, et al. Peroxiredoxin family proteins are key initiators of post-ischemic inflammation in the brain. *Nat Med* 2012; 18: 911–917.

41. Lehnardt S, Lachance C, Patrizi S, et al. The toll-like receptor TLR4 is necessary for lipopolysaccharide-induced oligodendrocyte injury in the CNS. *J Neurosci* 2002; 22: 2478-2486.

42. Lehnardt S, Massillon L, Follett P, et al. Activation of innate immunity in the CNS triggers neurodegeneration through a Toll-like receptor 4-dependent pathway. *Proc Natl Acad Sci USA* 2003; 100: 8514–8519.

43. Gorina R, Font-Nieves M, Márquez-Kisinousky L, et al. Astrocyte TLR4 activation induces a proinflammatory environment through the interplay between MyD88-dependent NFκB signaling, MAPK, and Jak1/Stat1 pathways. *Glia* 2011; 59: 242-255.

44. Shih RH and Yang CM. Induction of heme oxygenase-1 attenuates lipopolysaccharide-induced cyclooxygenase-2 expression in mouse brain endothelial cells. *J Neuroinflammation* 2010; 7: 86.

45. Verma S, Nakaoke R, Dohgu S, et al. Release of cytokines by brain endothelial cells: a polarized response to lipopolysaccharide. *Brain Behav Immun* 2006; 20: 449–455.

46. Leow-Dyke S, Allen C, Denes A, et al. Neuronal Toll-like receptor 4 signaling induces brain endothelial activation and neutrophil transmigration in vitro. *J Neuroinflammation* 2012; 9: 230.

47. Kettenmann H, Hanisch UK, Noda M, et al. Physiology of microglia. *Physiol Rev* 2011; 91: 461–553.

48. Bennett ML, Bennett FC, Liddelow SA, et al. New tools for studying microglia in the mouse and human CNS. *Proc Natl Acad Sci USA* 2016; 113: E1738-1746.

49. Zrzavy T, Machado-Santos J, Christine S, et al. Dominant role of microglial and macrophage innate immune responses in human ischemic infarcts. *Brain Pathol* 2018; 28: 791-805.

50. Banks WA and Erickson MA. The blood-brain barrier and immune function and dysfunction. *Neurobiol Dis* 2010; 37: 26–32.

51. Rosenzweig HL, Minami M, Lessov NS, et al. Endotoxin preconditioning protects against the

cytotoxic effects of TNFalpha after stroke: a novel role for TNFalpha in LPS-ischemic tolerance. *J Cereb Blood Flow Metab* 2007; 27: 1663-1674.

52. Orio M, Kunz A, Kawano T, et al. Lipopolysaccharide induces early tolerance to excitotoxicity via nitric oxide and cGMP. *Stroke* 2007; 38: 2812-2817.

53. Matsuda K, Tsuji H, Asahara T, et al. Sensitive quantitative detection of commensal bacteria by rRNA-targeted reverse transcription-PCR. *Appl Environ Microbiol* 2007; 73: 32–39.

54. Matsuda K, Tsuji H, Asahara T, et al. Establishment of an analytical system for the human fecal microbiota, based on reverse transcription-quantitative PCR targeting of multicopy rRNA molecules. *Appl Environ Microbiol* 2009; 75: 1961–1969.

Figure legends

Figure 1. Biological parameters of *db/+*, *db/db,* and polymyxin B (PL-B)-treated *db/db* mice measured prior to stroke induction with middle cerebral artery occlusion (MCAO). (a) Experimental design. (b) Plasma glucose levels (n = 5 per group). (c) Plasma levels of tumor necrosis factor (TNF)-α, interleukin (IL)-1β, and IL-6 (n = 5 per group). (d) Body weight (n = 6 per group). (e) Plasma lipopolysaccharide (LPS) levels (n = 6–9 per group). (f) Intestinal permeability assessed by quantitative analysis of fluorescein isothiocyanate (FITC)-dextran translocation (n = 5–6 per group). (g) Fecal bacterial counts analyzed by rRNA-targeted quantitative reverse transcription PCR (n = 5 per group). Bacterial counts below the threshold of detection were not plotted. Data are shown as mean ± SD. $*P < 0.05$, $**P < 0.01$, and $***P < 0.001$.

Figure 2. Biological parameters of *db/+*, *db/db,* and polymyxin B (PL-B)-treated *db/db* mice measured after stroke induction via middle cerebral artery occlusion (MCAO). (a) Plasma LPS levels after MCAO (n = 6–9 per group) (b) Intestinal permeability after MCAO (n = 5 per group). (c) Fecal bacterial counts after MCAO analyzed by rRNA-targeted quantitative reverse transcription PCR (n = 5 per group). Bacterial

counts below the threshold of detection were not plotted. Data are shown as mean ± SD. *$P < 0.05$, **$P < 0.01$, and ***$P < 0.001$.

Figure 3. Stroke outcomes in *db/+*, *db/db,* and polymyxin B (PL-B)-treated *db/db* mice. (a) Representative images of Cresyl Violet-stained brain sections (left) and quantification of infarct volumes (right) 24 h after middle cerebral artery occlusion (MCAO). Total hemispheric infarct volumes were corrected for edema (n = 8 per group). Scale bars = 1 mm. (b) Representative images (left) and quantification (right) of blood-brain barrier damage assessed by IgG immunoreactivity 24 h after MCAO (n = 5 per group). Scale bars = 1 mm. (c) Representative images of Iba1-positive cells, cell count of Iba1-positive cells, and percentage of Iba1-positive area in the peri-infarct area 24 h after MCAO (n = 4–6 per group). Scale bars = 20 μm. Data are shown as mean ± SD. (d) Double-immunofluorescence of Iba1 and anti-transmembrane protein 119 (TMEM119) in the peri-infarct area 24 h after MCAO in *db/+* and *db/db* mice. Scale bars = 20 μm. (e) Total number of TMEM119-positive cells and TMEM119-negative cells in Iba1-positive cells, and percentage of TMEM119-positive cells in Iba1-positive cells in the peri-infarct area 24 h after MCAO in *db/+* and *db/db* mice (n = 5 per group). (f) Modified neurological severity scores (NSS) 1 h and 24 h after

MCAO (n = 8 per group). Data are shown as median and interquartile range. (g) Seven-day survival after MCAO (n = 8–10 per group). Kaplan-Meier curve followed by the log rank test. (h) Infarct volumes 24 h after MCAO in polymyxin B-treated *db/db* mice with and without intraperitoneal lipopolysaccharide (LPS) administration. Total hemispheric infarct volumes were corrected for edema (n = 5 per group). (i) Cell count of Iba1-positive cells and percentage of Iba1-positive area in the peri-infarct area 24 h after MCAO in polymyxin B-treated *db/db* mice with and without intraperitoneal LPS administration. (n = 5 per group). Data are shown as mean ± SD. (j) Modified NSS 1 h and 24 h after MCAO in polymyxin B-treated *db/db* mice with and without intraperitoneal LPS administration (n = 5 per group). Data are shown as median and interquartile range. *$P < 0.05$, **$P < 0.01$, and ***$P < 0.001$.

Figure 4. Lipopolysaccharide (LPS), toll-like receptor (TLR) 4, and inflammatory cytokines in the ischemic hemispheres of *db/+*, *db/db,* and polymyxin B (PL-B)-treated *db/db* mice. Western blot analyses of (a) LPS and (b) TLR4 expression. (c) Enzyme-linked immunoassay results for tumor necrosis factor (TNF)-α, interleukin (IL)-1β, and IL-6. All data were analyzed in mice sacrificed 24 h after middle cerebral

artery occlusion (n = 5–10 per group). Data are shown as mean ± SD. *$P < 0.05$, **$P < 0.01$, and ***$P < 0.001$.

Figure 5. Cellular localization of lipopolysaccharide (LPS), *E. coli* K99 and toll-like receptor 4 (TLR4) in the peri-infarct areas of ischemic brain. Double-immunofluorescence of (a) LPS, (b) *E. coli* K99, and (c) TLR4 in microglia/macrophages (Iba1), neurons (NeuN), endothelial cells (CD31), and astrocytes (GFAP) in the peri-infarct area 24 h after transient middle cerebral artery occlusion in *db/db* mice. High magnification images show that (a) LPS and (b) *E. coli* K99 were adherent on the surface of microglia/macrophages, neurons and endothelial cells (arrows). (c) TLR4 was colocalized with Iba1, NeuN and CD31 (arrows). Scale bars = 20 μm. A red square in the brain illustration shows the region of analysis. (d) The percentages of TLR4-immunoreactive areas in Iba1, NeuN, and CD31-positive cells in *db/+*, *db/db*, and polymyxin B (PL-B)-treated *db/db* mice (n = 6 per group). Data are shown as mean ± SD. **$P < 0.01$ and ***$P < 0.001$.

Figure 6. Proposed mechanism of ischemic brain injury induced by metabolic endotoxemia. Gut dysbiosis in type 2 diabetes causes increased intestinal permeability and the translocation of microbiota-derived lipopolysaccharide (LPS) into the circulatory system. Disruption of the blood-brain barrier after cerebral ischemia allows an influx of LPS into brain parenchyma, where the induction of toll-like receptor 4 (TLR4), and inflammatory cytokines exacerbate ischemic brain injury.

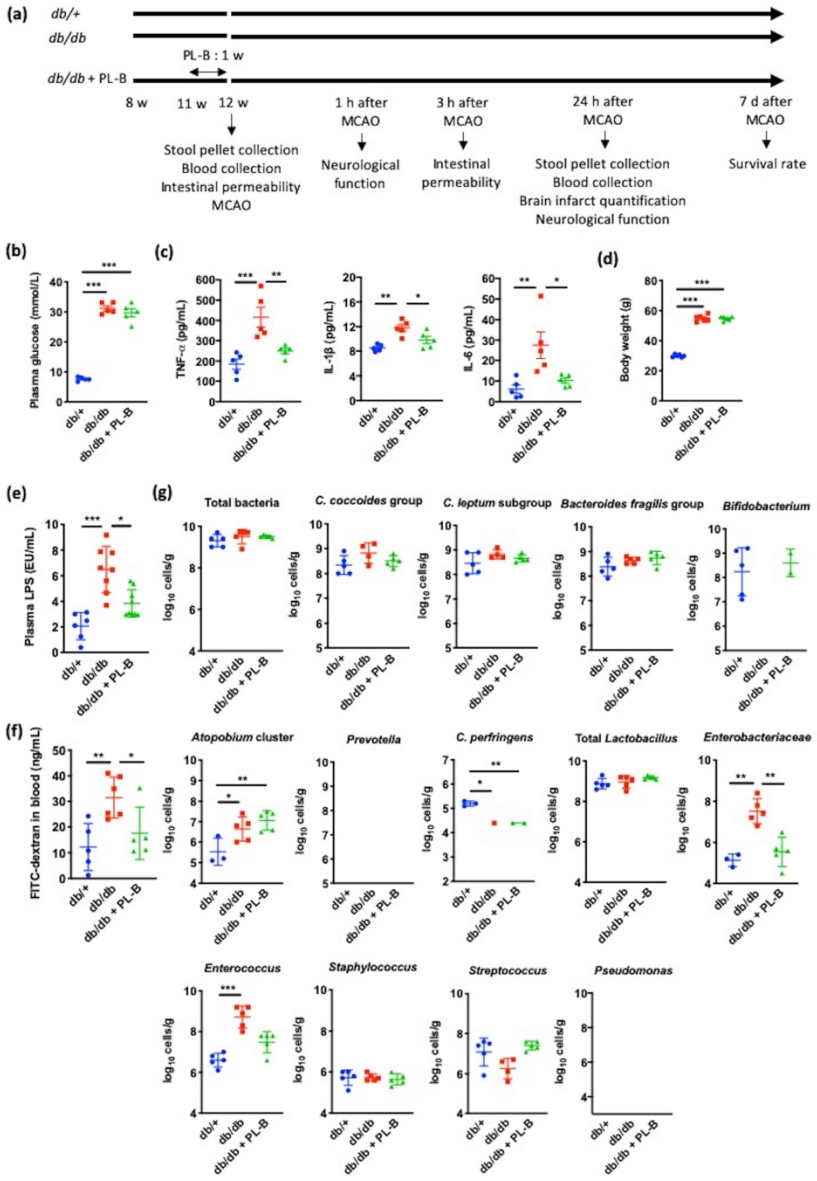

Figure 1

190x275mm (300 x 300 DPI)

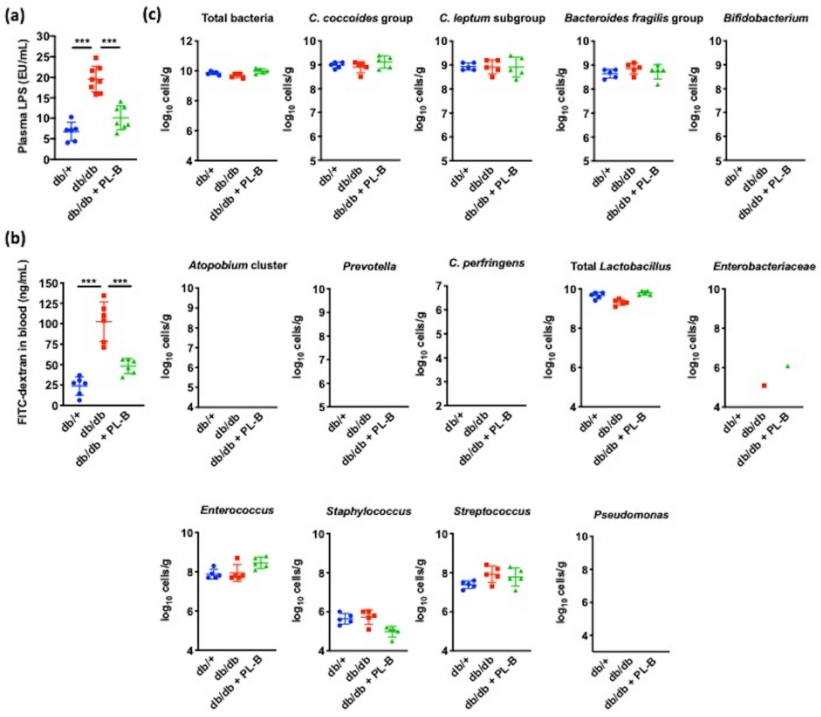

Figure 2

190x275mm (300 x 300 DPI)

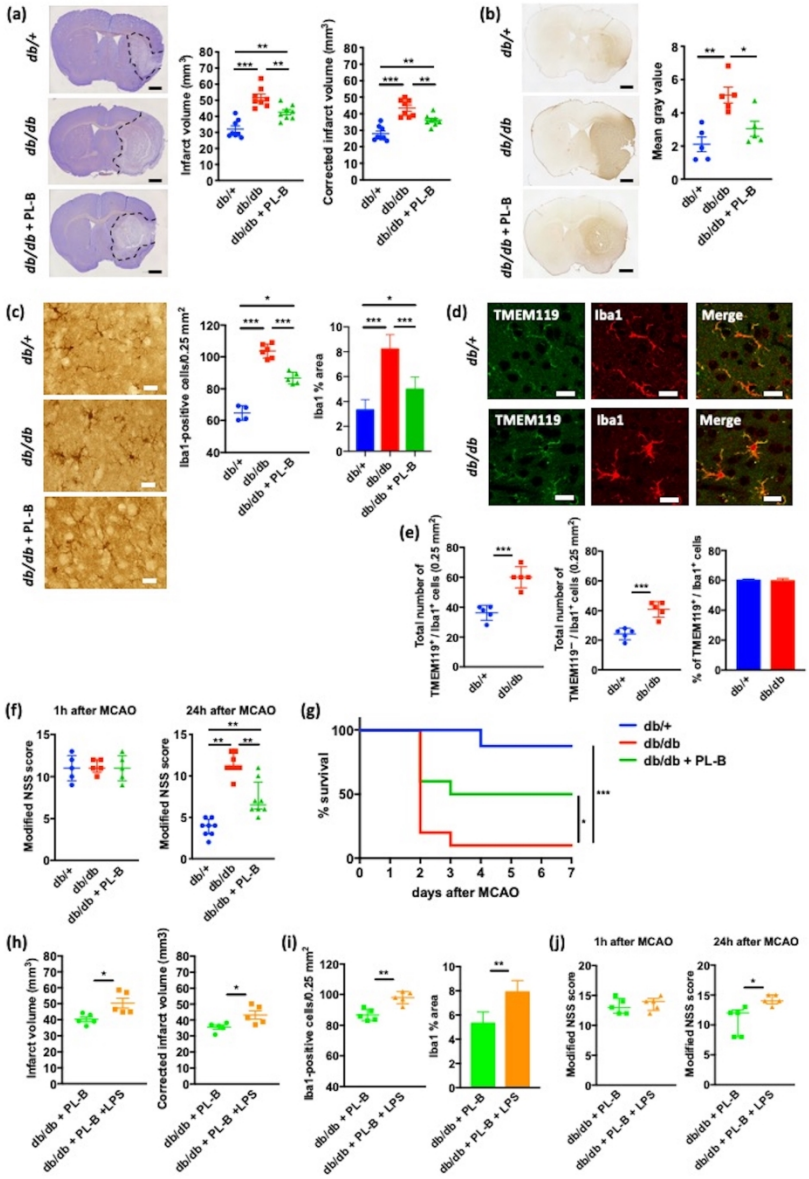

Figure 3

190x275mm (300 x 300 DPI)

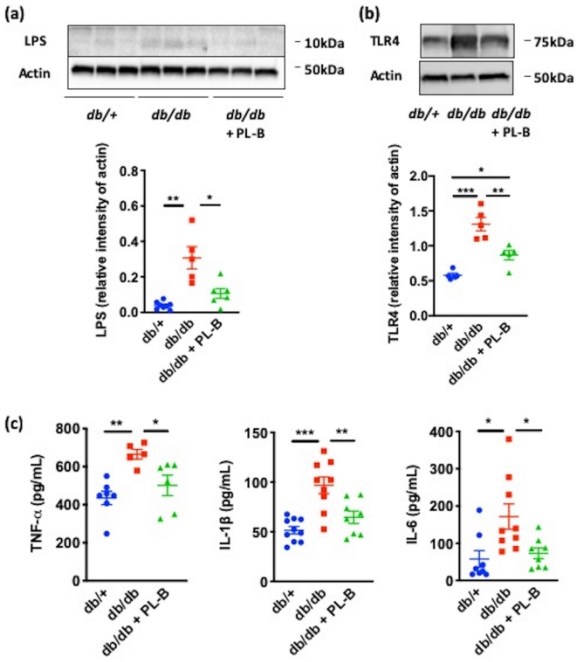

Figure 4

190x275mm (300 x 300 DPI)

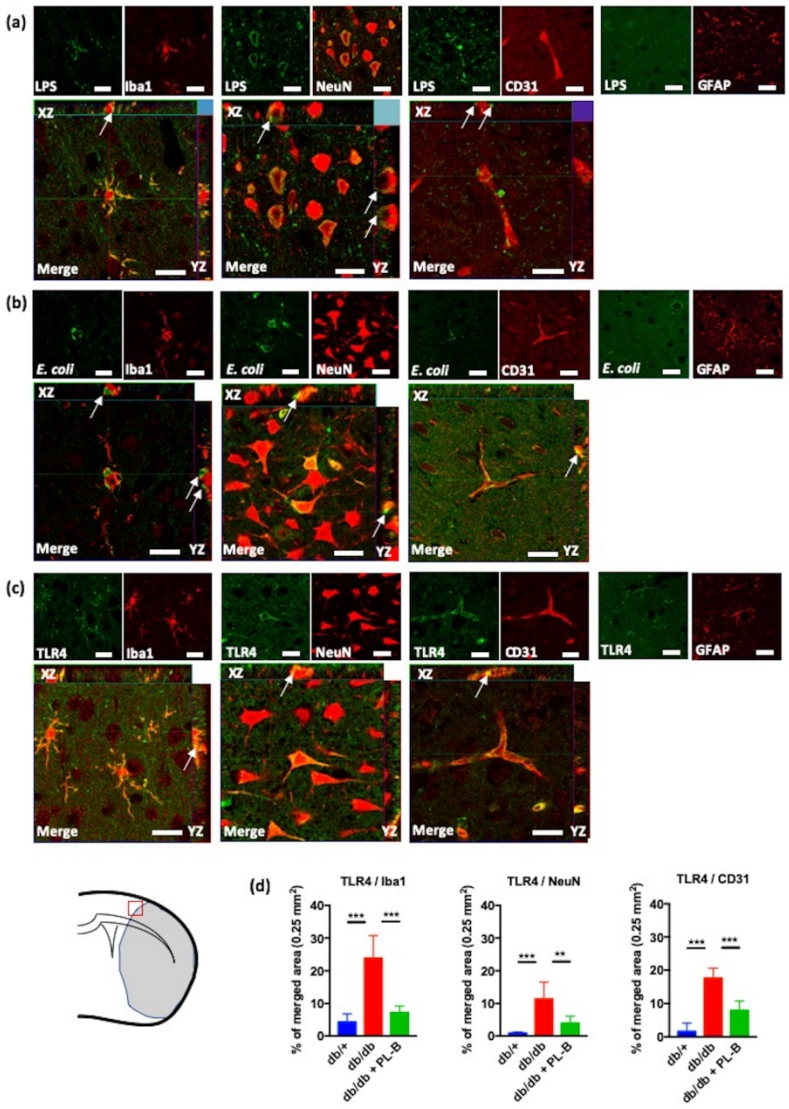

Figure 5

190x275mm (300 x 300 DPI)

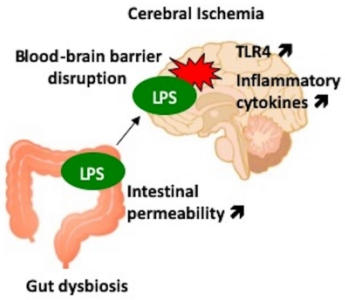

Figure 6

190x275mm (300 x 300 DPI)